RESEARCH ARTICLE

VOLCANICA

The episodic onset of explosive and silicic-dominated volcanism in a continental rift; insights from the Permian Oslo Rift, Norway

Jack W. Whattam *[α], Ivar Midtkandal[α], Dougal A. Jerram[βδ], Sara Callegaro[γε], and Henrik H. Svensen[αβ]

[α] Department of Geosciences, University of Oslo, Norway.
[β] Njord Centre, Department of Geosciences, University of Oslo, Norway.
[γ] Centre for Planetary Habitability (PHAB), Department of Geosciences, University of Oslo, Norway.
[δ] DougalEARTH Ltd., Solihull, UK.
[ε] Department of Biological, Geological, and Environmental Sciences, University of Bologna, Italy.

Abstract

The nature of rifting episodes and their associated volcanism mark key stratigraphic events in the evolution of volcano-sedimentary basins. Following the final assemblage of Pangea, the European region was subject to rifting and magmatism during crustal re-equilibration throughout the Permian. The aborted, partially eroded Oslo Rift is an excellent archive of this Permian magmatism, but the late-stage volcanological evolution is poorly understood. We present the first detailed documentation of a succession covering this period, with mafic lavas and volcaniclastic (tuff breccia) deposits, trachy-andesitic tuffs, and rheomorphic to moderately welded ignimbrites. Contrary to previous ideas, we show evidence suggesting the development of Strombolian-type scoria-cones, silicic fissure-fed eruptions, and major periods of rift-wide volcanic quiescence. Our observations highlight episodic silicic volcanism characterised by rapid evolution from high-grade ignimbrites to moderately and poorly welded ignimbrites. We infer rapid emptying of large, shallow silicic reservoirs and frequent source switching is responsible for the observed characteristics.

Keywords: Ignimbrite; Permian; Volcanic stratigraphy; Rift volcanism; Oslo Rift.

Submitted: 2024-01-29 | Accepted: 2024-09-23 | Published: 2024-12-13

Editor: F. Wadsworth | Typesetter: J. Farquharson

1 Introduction

Elucidating the magmatic evolution of rift settings presents a geological conundrum. Modern rifts provide a detailed record of recent volcanism but intrusive and older extrusive products are concealed. Ancient rifts present an opposing condition wherein the intrusive and older extrusive components are exposed but young deposits have been removed from the geological record due to post-magmatic uplift and erosion. For this reason, silicic volcanism (along with other late-stage volcanic components) is often an underestimated component of ancient rift settings, with patchy records commonly limited to sub-volcanic expressions (i.e. dikes and sills) and/or deeply-subsided intra-caldera deposits [Bryan et al. 2002; Tian et al. 2010; Swenton et al. 2022]. Through the late Carboniferous and early to middle Permian the European region was subject to a substantial period of post-orogenic crustal re-equilibration, rifting, and magmatism [Neumann et al. 2004]. The Permo-Carboniferous Oslo Rift (ca. 302–265 Ma) preserves an extensive record of both the extrusive and intrusive magmatic components related to this period. The stratigraphy, evolution, and origin of volcanism of the Oslo Rift (Figure 1A) was subject to intense study from the late 19th to late 20th century (starting with the pioneering work of Brøgger [e.g. Brøgger 1890]), with continued albeit less intensive study in recent years. Substantial volumes of work covering aspects of effusive eruptions, plutonic intrusions, and overarching theories of onset, development, and eventual decline of rifting and volcanism [e.g. Oftedahl 1946; Sæther 1947; Oftedahl 1978a; Ramberg and Larsen 1978; Neumann et al. 1985; 1988; Sundvoll et al. 1990; Olaussen et al. 1994; Rohrman et al. 1994; Sundvoll and Larsen 1994; Pedersen et al. 1995; Neumann et al. 2004; Ebbing et al. 2005; Andersen et al. 2011; Corfu and Larsen 2020]. However, despite considerable prior study, little is known of the late-stage volcanic and sedimentary activity, although these deposits could provide key information for understanding the timing and nature of late-stage intrusive complex formation.

Forming a coherent account of volcanic activity and evolution in regions the have undergone erosion, weathering, alteration, and deformation is challenging. Infilling (at least partially) of topographic lows [e.g. Branney and Kokelaar 1992; Bryan et al. 1998; Ebinghaus et al. 2014], diversion around and/or arrested flow against topographic highs [e.g. Pinkerton and Wilson 1994; Magnall et al. 2017], zones of non-deposition [e.g. bypassing zones: Brown and Branney 2004], interaction with and reworking within sedimentary and aqueous environments [e.g. Schneider et al. 2001; Bryan et al. 2002; Skilling et al. 2002; Manville et al. 2009; Ebinghaus et al. 2014; Sohn and Sohn 2019], transitions in activity within individual eruptions [e.g. Branney and Kokelaar 1992; Namiki and Manga 2008; Duraiswami et al. 2014; Wadsworth et al. 2020], and compositional heterogeneity within single eruptive units [e.g. Sumner and Branney 2002; Dreher et al. 2005; Czuppon et al. 2012; Willcock et al. 2015] all contribute to the complexity of volcanic stratigraphy. Volcano-tectonic faulting and deformation associated with caldera-collapse [e.g. Branney and Kokelaar 1994] and magmatic inflation respectively may introduce further complexity in intra-caldera settings, and where erosion

* jackww@uio.no

has erased the surficial volcanic and caldera structures the remnant features of faulting and inflation may be similar [e.g. arcuate faults and boundaries: Walker 1984; Branney 1995; Galland et al. 2022]. High resolution geological mapping and lithostratigraphical analysis are thus essential components for understanding the spatial and temporal evolution of these systems [Martí et al. 2018], and to provide the constraints necessary for interpreting geochemical and geochronological data in a geologically meaningful way.

New data opportunities from borehole and road-cut outcrops, improved age constraints [Corfu and Larsen 2020; Rämö et al. 2022], and advances in our understanding of volcanic and sub-volcanic systems [e.g. Sumner and Branney 2002; Brown and Branney 2004; Ross et al. 2005; Branney et al. 2007; Burchardt 2008; Galland et al. 2009; Tuffen et al. 2013; Brown et al. 2014; Mattsson et al. 2018; Galland et al. 2019; Sohn and Sohn 2019; Wadsworth et al. 2022] have prompted renewed interest and revisitation of fundamental aspects of the Oslo Rift. Furthermore, the Oslo Rift has exposures of a large proportion of the extrusive and intrusive components, permitting a fairly complete understanding of the magmatic evolution, thus presenting opportunities to study the contemporaneous volcanic and sub-volcanic evolution. In this study we focus on a volcano-sedimentary succession in the Alnsjø area (Figures 1 and 2), located in the north-eastern side of the city of Oslo, and at the southern limit of the Nittedal Caldera (called the Nittedal Cauldron in most prior literature: e.g. Naterstad [1978]). We present the results of systematic high-resolution geological mapping and lithostratigraphical analysis of a succession containing a major transition from dominantly mafic-effusive to dominantly silicic-explosive volcanism within the central portion of the Oslo Rift. Comprehensive fieldwork has indicated that ignimbrites are more common than previously thought (including rheomorhphic to lava-like varieties), and that basaltic volcanism also involved periods of explosive activity. Lithostratigraphic analysis did not provide evidence for caldera collapse during deposition of the ignimbrites. The stratigraphic record provides constraints on the relative timing, nature, and rapid compositional maturation of volcanism, and elucidates the varied style and composition of explosive volcanic activity in the central Oslo Rift. This succession thus constitutes an important stratigraphic record of volcanic evolution in a rift zone.

1.1 Geological Setting: the Oslo Rift

The Oslo Rift (Figure 1) is an aborted continental rift developed in the latest Carboniferous, culminating in the middle Permian, and is one part of a complex network of rift and graben segments in the Skagerrak-North Sea-Norwegian-Greenland Sea regions [Neumann et al. 1992; Neumann et al. 2004], and perhaps extending further south to France and the southern Alps [Locchi et al. 2022; Schulmann et al. 2022]. Collapse of the Hercynian-Variscan orogen and closure of the Palaeo-Tethys ocean is cited as the driver of widespread Permo-Carboniferous magmatism across Europe [Martí 1991; McCann et al. 2006; Larsen et al. 2008; Cassinis et al. 2011; Willcock et al. 2015]. An alternative (although not irreconcilable) theory suggests the earliest magmatic phase in the Oslo Rift (~300–299 Ma) was associated with a mantle plume impingement and Large Igneous Province (LIP) activity across Sweden, Germany, Scotland, England, and the North Sea, collectively termed the Skagerrak-Centred LIP [Torsvik et al. 2008].

The rift is roughly 520 km long and 35–65 km wide [Ramberg and Larsen 1978; Olaussen et al. 1994; Neumann et al. 2004; Larsen et al. 2008], comprised of the onshore Oslo Graben and offshore Skagerrak Graben, and is characterised by a low-degree of extension and large magmatic volumes [ca. 120,000 km^3, Neumann et al. 2004]. Rift activity spanned roughly 40 Myr from approximately 300 Ma to 262 Ma [Corfu and Larsen 2020], with uranium-lead (U-Pb) dating and stratigraphic correlations indicating a general north to south progression of magmatism [Corfu and Dahlgren 2008; Larsen et al. 2008]. The rift stratigraphy is partitioned into six key stages. Deposition of the dominantly fluvial and lacustrine Asker Group sediments dominated the proto-rift [stage 1: Olaussen et al. 1994; Larsen et al. 2008] with some syenitic and ultramafic sill intrusions [Sundvoll and Larsen 1994]. Sill intrusions have radiometric rubidium-strontium (Rb-Sr) ages in the range 308–305 Ma [Sundvoll et al. 1992; Larsen et al. 2008]. Initial rifting (stage 2) was accompanied by alkaline to tholeiitic mafic magmatism at ca. 300 Ma [Corfu and Dahlgren 2008], first as relatively thin (~0.5–5 m) flows, and later as thicker flows up to ca. 10 m thick, forming a lava-complex up to 1500 m thick in the central rift [Larsen et al. 2008], but thinning to 10s of metres to the north [Neumann et al. 2004]. The eruption of substantial volumes of trachyandesitic rhomb-porphyry lava characterised the climactic rift phase (stage 3) and overlapped with the basaltic eruptions of stage 2. Early rhomb-porphyry lavas were thick and relatively extensive flows with volumes of up to 1000 km^3 and areal coverage of roughly 10,000 km^2 [Larsen et al. 2008]. The total lava-pile for the Rhomb-Porphyry series varies across the rift, with an approximate maximum thickness of 3 km in the southern portion of the Oslo Graben, and approximately 900 m to the north-west of Oslo. Sediments were deposited as thin interstitial deposits between individual lava flows [Larsen et al. 2008], and as larger packages above lava flows [e.g. the Brummunddal sandstone, Andersen et al. 2011]. Stages 2 and 3 were accompanied by the emplacement of larvikite batholiths [Larsen et al. 2008] with ages ranging from ca. 302–289 Ma [Dahlgren et al. 1996; Corfu and Dahlgren 2008; Rämö et al. 2022] in the south to ca. 281–277 Ma in the central rift portion [Pedersen et al. 1995]. The middle to late transitional stage [stage 4: Larsen et al. 2008] is typically discussed as a period of central-volcano formation and caldera forming explosive eruptions [Sæther 1962; Neumann et al. 1992; Larsen et al. 2008], as evidenced by the juxtaposition of distinctly different rock types along circular boundaries suggested to be caldera ring faults [Segalstad 1975; Oftedahl 1978b], and by the presence of volcaniclastic deposits within these circular features [Oftedahl 1978a]. Volcanic activity is inferred to have produced 18 caldera structures (Figure 1A and 1B) over a rift length of roughly 180 km [Oftedahl 1978a] during this stage. Ages for caldera or caldera-related deposits are sparse but recent U-Pb dating in the northern Oslo Graben suggests a concentrated period of activity

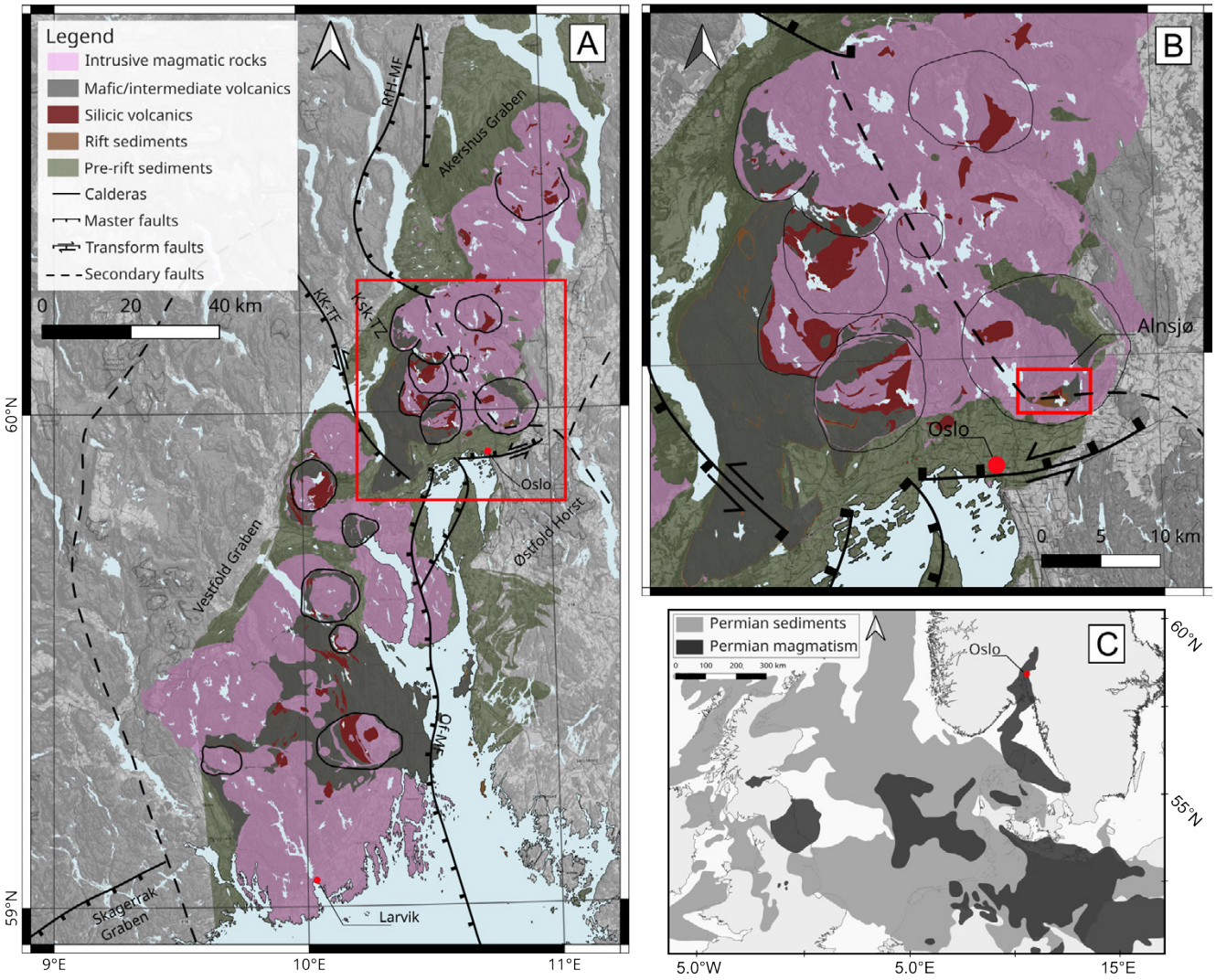

Figure 1: [A] and [B] show simplified geology and major structural features of the Oslo Rift (after Larsen et al. [2008] and Sundvoll and Larsen [1994]). [B] is an enlargement of the red box in [A] showing the central rift and Alnsjø areas relevant to this study. [C] Approximate distribution of Permian-age sedimentary and magmatic deposits across north-western Europe (after Heeremans and Faleide [2004] and McCann et al. [2006]). Abbreviations in [A] are: Oslofjord Master Fault (Of-MF); Krokkleiva-Kjaglidalen Transfer Fault (KK-TF); Krokskogen Transfer Zone (Ksk-TZ); Randsfjorden-Hunnselv Master Fault (RfH-MF)

between ca. 276–273 Ma for silicic eruptions and contemporaneous construction of intrusive complexes in this region [Corfu and Larsen 2020]. Small volume (0.1–1 km diameter) alkaline-gabbros and larger granitic batholiths were intruded in the end phases of stage 4 [Neumann et al. 1985; Larsen et al. 2008]. The Alnsjø area, targeted by this study is suggested to recorded activity during this stage [Sæther 1946; Naterstad 1978; Larsen et al. 2008]. The final two stages were dominated by emplacement of syenitic to granitic plutons at ca. 265–260 Ma, along with widespread emplacement of syenitic, rhomb-porphyry, and diabase composition dykes in the termination stage [Larsen et al. 2008; Corfu and Larsen 2020].

1.2 Geological setting: the Alnsjø region

The study region (Alnsjø, Figure 2) is located at the north-eastern edge of Oslo and is situated at the southern edge of the Nittedal Cauldron in the northern portion of the Oslo Graben [Naterstad 1978]. The area is surrounded by syenite and alkali-feldspar syenite, and the southern crescent-shaped boundary is suggested to represent the ring fault of the Nittedal Cauldron [Sæther 1946]. The Alnsjø succession is suggested to host the youngest volcanic and sedimentary deposits in the rift [Sæther 1946; Naterstad 1978], with basaltic lavas observed as the basal unit in the area, and are overlain by basaltic sediments, rhyolites and volcanic breccias, mudstone (argilite), and an alluvial conglomerate. Subsequent deformation has formed a synclinal structure, previously described as a boat-shaped syn-

cline [Naterstad 1978], with a dominant north-south folding, and lesser east-west folding. Caldera subsidence on the order of 800–1000 m and later emplacement of a plutonic body is the inferred cause of the synclinal structure [Naterstad 1978].

2 Methods

Fieldwork was conducted over the summer periods of 2021–2023. Outcrops in the field area are of extremely variable quality (e.g. degree of weathering, exposure, plant cover), and some units a substantially underrepresented with regards to outcropping area. Deposits characteristics and variations, including unit thickness, stratification, bedding orientations, clast and/or phenocryst characteristics, welding features and degree, contact features (where visible), were defined using >700 outcrop observation points (observation point coverage is detailed in Supplementary Material 1). Stratigraphic logs were collected in locations containing the best outcrop exposures and most continuous successions. Therefore, stratigraphic logs are amalgamations of the best (and most accessible) outcrops and often required substantial lateral shifts to cover gaps where there was no outcrop exposure Geological mapping was conducted at approximately 1:25,000 scale using the publicly available Norges geologiske undersokelse (NGU, the Norwegian Geological Survey) geological map* as a base reference, with observation locations and outcrop details recorded in Mergin Maps [v2.1.0: Mizera et al. 2022] with a handheld global positioning system (GPS). Geospatial data was transferred to `QGIS` [Quantum Geographic Information System: QGIS Development Team 2009] for detailed map construction and attribute data management (e.g. sample location data and structural measurement data and locality). `QPROF` [Alberti and Zanieri 2023], a `QGIS` plugin, was used in combination with LiDAR point cloud data sourced from Kartverket (Norwegian Mapping Authority) to construct high resolution cross-sections through the mapped area and features. Many volcanic deposits exhibited variable and/or convolute stratification and as such were unreliable units for structural measurements. Additionally, the thickest sedimentary unit was dominantly unstratified; therefore the majority of structural data was collected in a small portion of the total sedimentary deposits. Sampling was undertaken during mapping and stratigraphic logging of sections.

3 Naming and nomenclature

Several of the units described below are not discussed or named in prior literature; the description and mapping of this area given by Naterstad [1978] is the most recent and complete work covering the Alnsjø succession prior to this contribution. With regard to unit names, simple designations such as B1 (e.g. basalt flow number 1) have a long-standing history of use in the Oslo Rift for denoting packages of basalts (B1, B2, and B3) and rhomb-porphyry (R1-RP15) lavas [e.g. Larsen et al. 2008]. Basalts B1 and B2 are clearly separated by the rhomb-porphyry lavas, with B1 occurring before and B2 within. B3 (and B4–B5 where mentioned) are less clearly defined in the literature but B3 is typically thought to occur before RP13, with B4 and B5 being used for local occurrences of basalts above RP13. Distinction and numbering of the rhomb-porphyry is applied based on unique phenocryst assemblages (summary in Oftedahl [1978a]). The rhomb-porphyry stratigraphy has largely been constructed from the Krokskogen area (Figure 1) and may not be accurate across the entire rift. In the absence of new geochemical data we have used compositional terms such as basalt and trachy-andesite in line with what is known of the overall stratigraphy of the Oslo Rift and the Alnsjø region. To avoid confusion with previous literature and the established designations outlined above we herein use a convention of general location and lithology to name lithostratigraphic units. Furthermore, the succession is hereinafter split into four primary subsections (phases) based on marked changes in the volcanic and sedimentary characteristics.

In the basaltic units, we use domain, bomb, and spatter as descriptive terms. Domain refers to regions within lava flows with sharp boundaries and a distinct phenocryst assemblage from that of the surrounding material. Bomb and spatter both refer to clasts >64 mm in size with characteristics indicative of ductile or fluidal behaviour within a granular or volcaniclastic groundmass, wherein bomb and spatter denote clasts with lmited or substantial flattening respectively. We use the terminology relating to pyroclastic deposits (e.g. rhemorphic, lava-like, lapilli tuff, tuff breccia) after Branney and Kokelaar [2002] and White and Houghton [2006]. Tuff breccia in particular is used for deposits (here only mafic varieties) comprised of angular to sub-rounded blocks/bombs, lapilli, ash, and lithics, with variable proportions of agglomerate facies [e.g. fluidal lapilli or spatter: Branney and Kokelaar 2002]. Welding is used qualitatively to denote pyroclastic deposits that have undergone syn- or post-depositional compaction and sintering of clasts while in a hot, ductile state. Welding degree is used qualitatively after Walker [1983] and Branney and Kokelaar [1992]. Unwelded denotes deposits with clear granular groundmass, and relatively undeformed clasts; moderately welded denotes deposits with a well-developed eutaxitic texture in a granular groundmass; and densely welded denotes deposits with no visible remnant granular groundmass texture, very well-developed eutaxitic textures, flow banding, or almost no relict clast textures [i.e. lava-like ignimbrites: Branney and Kokelaar 1992; Andrews and Branney 2010]. Peperite is used in the genetic sense after White et al. [2000] and does not imply extrusive or intrusive origins, but is taken as indication of interaction between hot magmatic or volcanic material and unconsolidated or partially-consolidated deposits.

4 Results

The distribution of syenite, granite, and nordmakite surrounding the study area (Figure 2) was taken from existing geological maps available through NGU [Lutro and Nordgulen 2008]. These were not re-mapped or investigated in detail during fieldwork as they significantly post-date the Alnsjø succession. Several dikes also cross-cut the area but are not shown as they post-date the volcano-sedimentary succession and most cannot be followed beyond a single outcrop exposure. Two key features are however worthy of mention in relation to the overall interpretation of the area: 1) 300–500 m

*Available at `https://www.ngu.no/geologiske-kart`

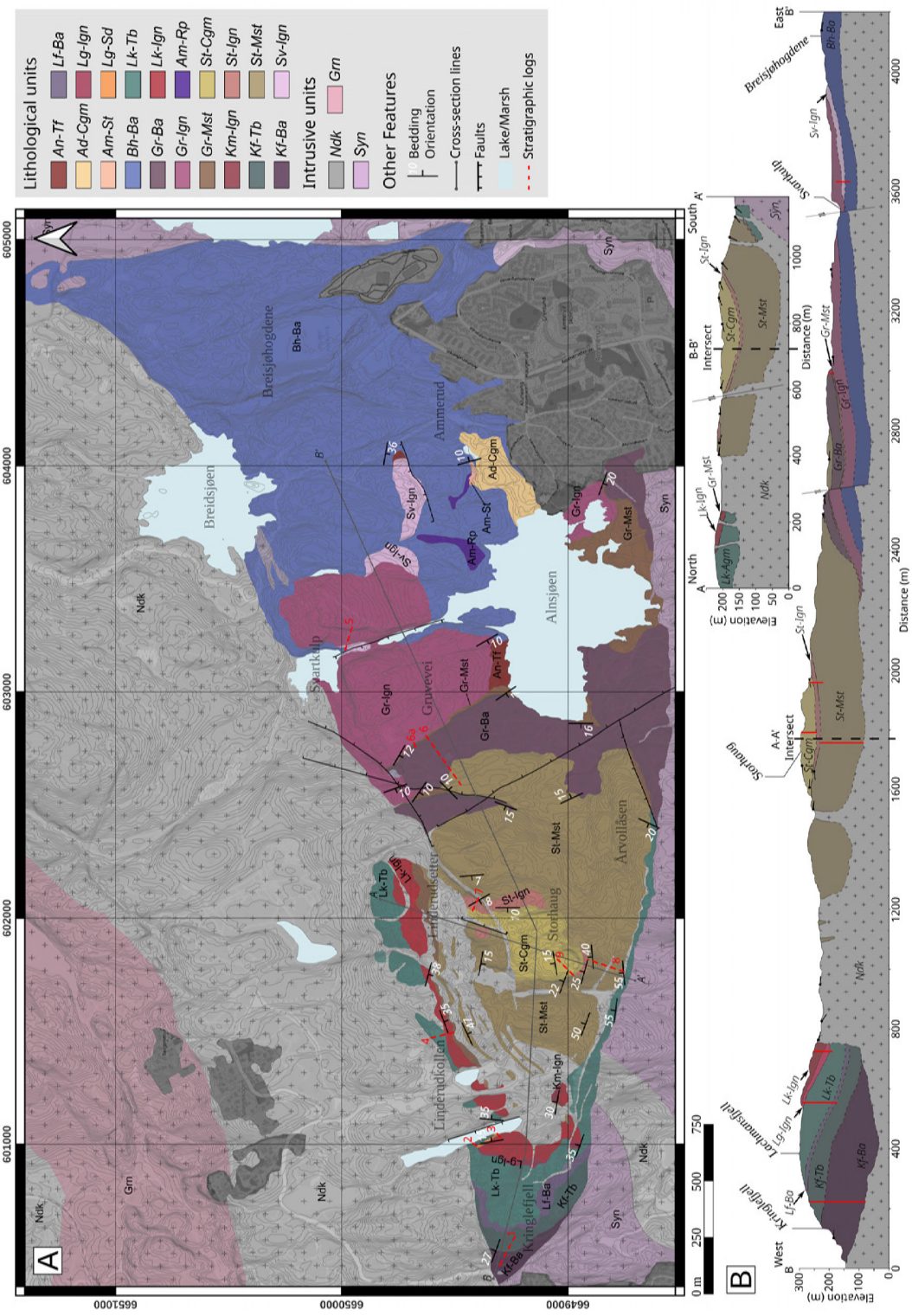

Figure 2: Summary of geological mapping, lithostratigraphy, and interpreted geological cross-sections of Alnsjø area: [A] Geological map showing the interpreted distribution of volcanic and sedimentary units across the study region, including structural measurements and inferred faults; [B] geological cross-sections running north-south (B–B') and east-west (A–A') showing general synclinal structure interpreted from structural measurements shown in 1a. Unit names are abbreviated for simplicity and are given in full in Table 1 below. Lithology abbreviations in unit names are as follows: tuff (Tf), basalt (Ba), ignimbrite (Ign), conglomerate (Cgm), sandstone (St), tuff breccia (Tb), mudstone (Mst), rhomb porphyry (Rp), nordmakite (Ndk), granite (Grn), and syenite (Syn).

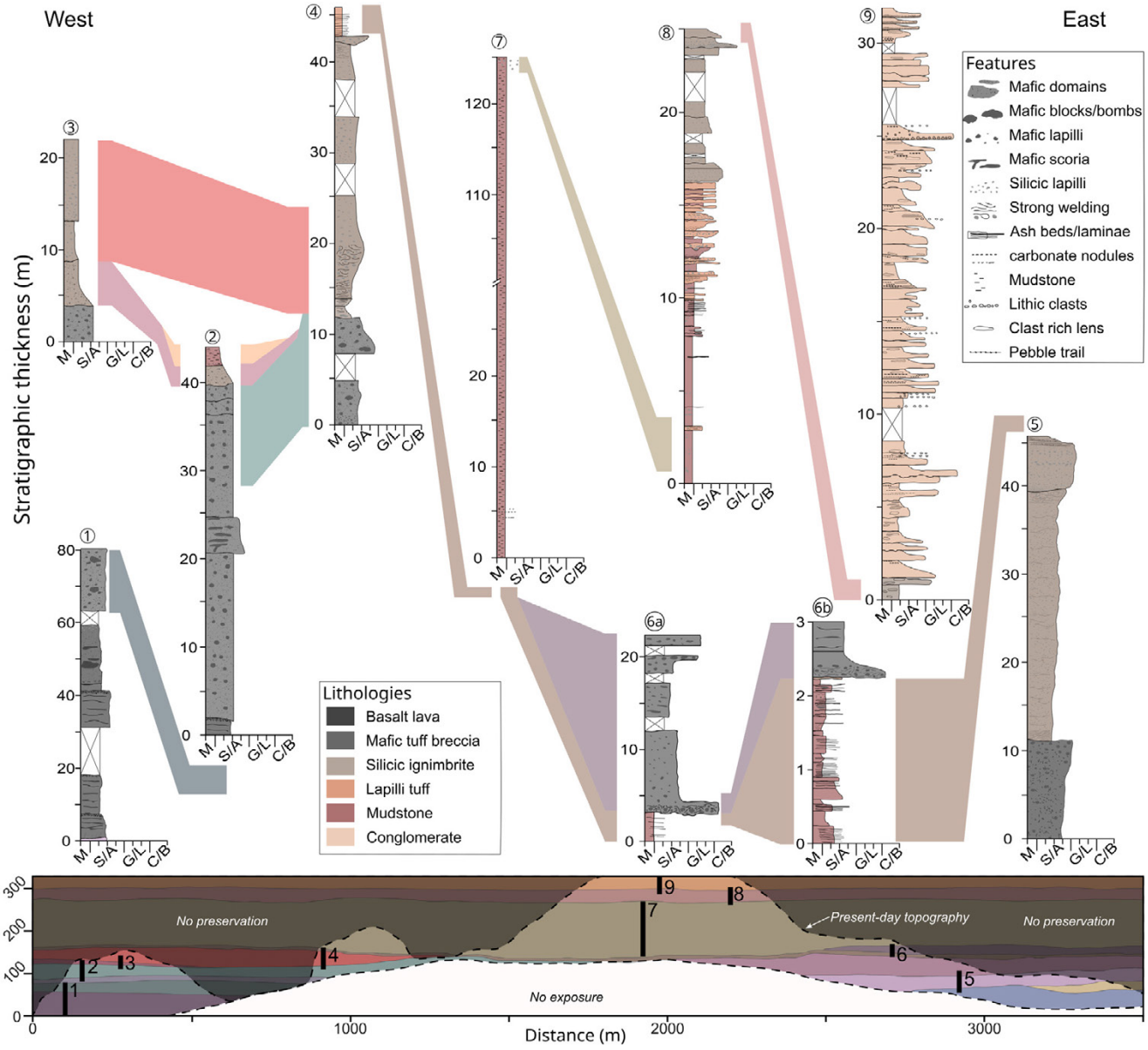

Figure 3: Stratigraphic logs collected in the Alnsjø field (above) and an approximation of the undeformed Alnsjø geology (below). Logs are shown in geographical (west to east) order, with coloured polygons showing approximate correlations and/or relative vertical position of logs. Note scale differences in log numbers 1, 5, 6b, 8, and 9. m - mud, S/A - sand/ash, G/L - gravel/lapilli, and C/B - cobble/bomb/block in the abbreviated grain-size scale. Colours correspond to those shown in the legend in Figure 2, although not all mapped units are represented in the stratigraphic logs. Relative positioning and coverage of stratigraphic logs is shown in the simplified section as vertical black lines.

south of the boundary of the volcano-sedimentary succession we noted angled syenite dikes (dipping ca. 65replaced—70 degrees north) with strikes roughly parallel to the southern boundary of the study area; 2) a ca. 2 × 5 m inclusion of an accretionary lapilli ash is present within the syenitic intrusive complex to the south-west of the mapped area (Figure 2B and 2C) and is texturally equivalent to a similar-sized inclusion in the lowermost western basalt (see Figure 4, and Kringlefjell Basalts in Table 1 and Supplementary Material 1). Deposition of the volcano-sedimentary succession was followed by emplacement of dominantly silicic (granite, syenite, and nordmakite, and alkali-feldspar syenite) intrusive complexes during the penultimate magmatic phase of the Oslo Rift [e.g. Naterstad 1978; Larsen et al. 2008] and associated con-

tact metamorphism has caused varying degrees of alteration to both volcanic and sedimentary facies throughout the succession. Chlorite, calcite, and epidote are typically observed in outcrop and hand-sample, suggesting zeolite to greenschist grade contact metamorphism. However, detailed characterisation of metamorphic alterations is beyond the scope of this contribution and is not further considered.

4.1 Mapping, structure, and stratigraphy

A revised geological map (Figure 2A) has been constructed based on detailed outcrop observations (see Supplementary Material 1) and nine stratigraphic logs (Figure 3) collected in key locations with the greatest exposure of lithologies. Marked differences in the lower ca. 115–130 m of stratigraphy are present between the east and west, although overall changes in volcanic style are consistent across the entire area. In previous maps [e.g. Naterstad 1978], several distinct basalt and basaltic agglomerate units were grouped, some pyroclastic or rubbly flow top portions of basaltic units were mapped separately from their coherent core sections, and several texturally and compositionally distinct silicic ignimbrites were grouped.

In addition, mapping the area in greater-detail (and with the aid of modern GPS tools and LiDaR topographical data) has shown that odd features (e.g. straight/angular boundaries, and circular exposures) in previous geological maps [Naterstad 1978] are misinterpretations, likely resulting from low-resolution mapping.

Two cross-sections, running approximately east-west (A–A': Figure 2B) and north-south (B–B': Figure 2C), have been cut through the updated map. Structural measurements indicate an overall synclinal structure (Figure 2A) which is schematically interpreted in cross-section (Figure 2B). Structural measurements also highlight comparatively gentle eastward and westward dipping limbs (Figure 2C). Based on the irregularity of the relationship between intrusive syenitic rocks and the volcanic and sedimentary units, the cross-sections present a heavily simplified and schematic representation of this relationship. Whilst some previously mapped faults were removed due to lack of convincing field evidence, we have also added some new inferred faults based on juxtaposition of distinct units on either side of syenitic dykes. Vertical or horizontal offsets on these inferred faults are on the order of a few metres to less than ten metres, although accurate estimation is hindered by lack of clear marker beds in many of the faulted units.

4.2 Lithofacies of the Alnsjø field

The Alnsjø field succession comprises a complex and variably preserved sequence of lithofacies. A summary of lithofacies, interpretations of the volcanic or sedimentary origins and depositional style, and inferred rift activity is given in Table 1 below. The detailed descriptions and interpretations of each unit are provided in Supplementary Material 1.

5 Discussion

5.1 Geological development

Geological mapping, stratigraphic reconstruction, lithofacies descriptions, and structural information, in combination with broad correlations across the wider Krokskogen transfer zone area (Figure 1B) allow for reconstruction of the volcanic and sedimentary evolution in the central rift. Simplification and correlation between eastern and western stratigraphic sections (Figure 8) highlights key boundaries defining changes in the style of volcanism and/or volcanic hiatuses where sedimentary erosion and deposition was dominant. Phases are constrained by these boundaries and the generalised volcano-sedimentary evolution is depiction in a schematic four phase model (Figure 9).

5.1.1 Pre-eruptive landscape

Fissure-fed basaltic and trachy-andesitic (rhomb-porphyry) eruptions characterised the early- to middle-stage rift activity [Larsen et al. 2008]. Typically minor alluvial, aeolian, and lacustrine deposits are intercalated within the lava pile [Henningsmoen 1978; Olaussen et al. 1994], with one example of a thick (ca. 150 m) rhomb-porphyry conglomerate infilling erosional topography in northern Krokskogen. Along the Oslofjord master fault large (ca. 1000 m thick) alluvial fans accumulated. Alongside the initiation of the central volcano phase, tectonic activity is suggested to have slowed and the dominant structural orientation switched from a broadly N–S to E–W alignment [Neumann et al. 2006]. Late-Carboniferous to late-Permian plate reconstructions place North-western Europe and Fennoscandia near the palaeo-equator, at approximately 10–20 degrees north [Torsvik and Cocks 2004; Torsvik et al. 2008], with tropical semi-arid to arid conditions reported for similar latitudes across the middle and late Permian [DiMichele et al. 2001; Benton 2018; Gibson and Wellman 2021]. The pre-eruptive environment is therefore envisioned as a seasonally wet, semi-arid to arid setting with a low to moderate relief topography formed by partially eroded lava flows, with minor silicic ash deposits and small pockets of fine sediments infilling topographic lows. Tectonically formed relief was likely significant along N–S trending rift master faults but lava flows likely infilled tectonic lows within rift valleys.

5.1.2 *Phase 1*

Phase 1 comprises basalt lava flows overlain by pyroclastic basaltic deposits. However, some small-volume silicic eruptions did precede the phase 1 basalts, evidenced by the large inclusion of accretionary lapilli ash in the lowermost Kringlefjell basalt. The lower three Kringlefjell lava's basalt lava flows appear to be simple pāhoehoe type flows [e.g. Barreto et al. 2014] with minor intra-flow stratification. Preservation of rubbly flows tops and a lack of evidence for sedimentary deposits or paleosols in between the western lava flows suggests relatively short inter-eruption periods. Moderate flow thicknesses, presence of rubbly flow-tops, dense core zones, and consistent phenocryst assemblages within each unit indicates these were moderate-volume inflated pāhoehoe-type flows likely sourced from distinct magma reservoirs (suggested by distinct phenocryst populations). Overlying basaltic

Table 1: Summary of lithostratigraphic units, eruptive and depositional interpretations, and development of overall rift activity.

Phase	Lithology	Units	Unit Abrv.	Spatial distribution	Description
Phase 1	Basaltic lavas	Breisjøhogdene Basalt	Bh-Ba	Basal unit across the eastern region of Alnsjø. Limited vertical exposure (<15m). Present at same stratigraphic level as Kringlefjell Basalts in the west.	Typically coarse porphyritic basalt, with large (4–15 mm) tabular plagioclase phenocrysts. Some outcrops have amygdules (chlorite filled), and upper portions (near contact with Svartkulp Ignimbrite (see phase 2) are often clastogenic (agglomerate).
		Kringlefjell Basalt (K1, K2, & K3)	Kf-Ba	Exposed in and marking the base of the succesion in west Alnsjø. Total thickness of ca. 60 m with individual flows 10–15 m thick.	Three basaltic lava flows, coarse porphyritic (K1 and K3) and aphyric (K2) with subtle indications of internal flow stratification. Phenocrysts in K1 and K3 are 1–6 mm tabular plagioclase, with moderately common occurence of plagioclase glomerocrysts. Flow tops are heavily erode but small (<1 × 1 m) outcrops display rubbly and brecciated textures.
		Kringlefjell Basalt (K4)			Aphanitic to aphyric basalt lava hosting large (<50 cm to <4 m) domains of coarse-porphyritic basalt. Coarse domains have textures such as phenocryst alignment with domain boudanries, incipient breakout lobes, and cuspate margins that indicate fluidal (i.e. ductile) behaviour during deposition.
	Pyroclastic basalt	Kringlefjell Tuff Breccia*	Kf-Tb	Only found in the far west directly overlying the Kringfjell Basalts. Generally poorly exposed, with approximate thickness of 15 m**	Unstratified to crudley stratified pyroclastic basalts with and occasional lava flows. Clast populations can be unimodal or bimodal, are dominantly porphyritic, vesicular to non-vesicular basalt, with less common scoria, and rare vesicular felsic clasts. Many larger clasts show in-situ disaggregation textures. Groundmass typically comprised of ash size material and phenocrysts of similar size to those in porphyritic clasts. Clasts are typically amoeboidal or rounded to sub-rounded shapes, but sub-angular clasts occur in some deposits.
	Basaltic Lava	Lachmansfjell Basalt*	Lf-Ba	Only exposed in the far west of Alnsjø in sparse thin (1–3 m) outcrops. Topography at outcrop locations indicates likely total thickness of ca. 8–10 m**	Thin (ca. <10 m thick) coarse porphyritic basalt with moderate content (ca. 10–15 %) of pagioclase phenocrysts, and a poorply to non-vesicular groundmass.
	Pyroclastic basalt	Linderudkollen Tuff Breccia	Lk-Tb	Found through the west and middle regions of Alnsjø, where it marks the base of the preserved succession. No continuous exposure of entire unit, but multitude smaller, high-quality outcrops distribute across the west and central areas. Thickness of ca. 35–40 m	Unstratified to crudley stratified pyroclastic basalts with and occasional lava flows. Clast populations can be unimodal or bimodal, are dominantly porphyritic, vesicular to non-vesicular basalt, with less common scoria, and rare vesicular felsic clasts. Many larger clasts show in-situ disaggregation textures. Groundmass comprises dominantly angular ash, fine lapilli, and fragmented phenocrysts of similar size to those in porphyritic clasts. Clasts are a mixture of sub-rounded and amoeboidal shapes, with some sub-angular clasts.

Table 1 (continued): Summary of lithostratigraphic units, eruptive and depositional interpretations, and development of overall rift activity.

Phase	Lithology	Units	Unit Abrv.	Spatial distribution	Description
Phase 1 continued	Basalt derived sediments	Ammerud Sandstone*, AllundammenConglomerate*	Am-St, Ad-Cgm	These units have very limited preservation (one outcrop location per unit) in the far east of Alnsjø. Sandstone has preserved thickness of ca. 5 m, other units unknown.**	Sandstone is medium to coarse grained, with planar stratification. Conglomerate only exposed in flat-lying sections (i.e. bedding features not visible) but appears to be poorly sorted, matrix supported, with rounded to well rounded ca. 3-15cm clasts. Clasts are dominantly basaltic varieties with subsidiary rhomb-porphyry population (<10 %).
	Lava feeding magmatic conduit	Ammerud rhomb-porphyry	Am-Rp	Two occurences in east Alnsjo with steep (ca. 70–75°) cross-cutting contacts with the Breisjøhogdene basalt and Ammerud Sandstone.	Dark red to black, coarse porphyritic trachy-andesite with ca. 8–17 mm rhomb shaped plagioclase phenocrysts. Slightly vesicular and occasionally clastogenic. One outcrop exposes a clast and ash rich zone along contact zone with the Breisjøhogdene Basalt, with clasts of rhomb-porphyry and the host basalt, in a red ash-rich groundmass.
	Moderately welded lapilli tuff	Alsnjø Tuff	An-Tf	Overlies the Breisjøhogdene Basalt in east Alnsjø with very limited preservation. Minimum thickness of 5 m.	Reddish coloured ash rich moderately welded, stratified fine lapilli tuff, with sparse lithics. Invariably matrix supported, with planar- and cross-statifcation, and a bimodal clast-size distribution is bimodal dominated by fine lapilli (<2cm) with sparse large lithics (ca. 5–25 cm length). Lithic blocks are rounded with partially foamed edges. Broadly compositionally equivalent to rhomb-porphyry units (trachy-andesite).
Phase 2	Moderately welded ignimbrite	Kringlefjell Ignimbrite*,**	N/A	One ~2 m thick outcrop in the far west overlying the Kringlefjell Tuff Breccia.**	Unstratified lapilli tuff, with rotated lapilli and moderate to poorly developed fiamme.
	Densely welded ignimbrites	Svartkulp Ignimbrite	Sv-Ign	Found overlying the Breisjøhogdene Basalt in the east with a continuous 25 m exposure at the lake Svartkulp. Other exposures are patchy in flat lying terrain.	Densely welded (i.e. lava-like) diffuse stratified, crystal-rich ignimbrite, displaying subtle planar to slightly convolute flow-banding. Basal ca. 1 m displays fine (<5mm thick) highly elongate fiamme and sparse fine (<1 cm) rounded lithics.

Table 1 (continued): Summary of lithostratigraphic units, eruptive and depositional interpretations, and development of overall rift activity.

Phase	Lithology	Units	Unit Abrv.	Spatial distribution	Description
Phase 2 continued	Densely welded ignimbrites	Linderudkollen Ignimbrite	Lk-Ign	Overlies the Linderudkollen Tuff Breccia in the north and west. Very good ca. 30 m thick, semi-continuous exposure in the north-west (at Linderudkollen)	Densely to moderately welded stratified ignimbrite, displaying planar to convolute flow banding, fiamme, deformed and elongated vesicles, rotated clasts and associated deformed flow-banding, with a sharp, undulating lower contact. Basal 30–40 cm thick moderately to highly vesicular pumiceous layer is overlain by 6 m thick lava-like to rheomorphic region, which rapidly transitions to a moderately welded to unwelded upper 10-3m thick region. Lava-like portion has stretched and flattend vesicles but no clear pyroclastic textures whereas rheomorphic portion has a poorly sorted ash-rich to glassy groundmass with abundant crystals, rotated clasts, and sparse xenolithic inclusions (coarse porphyritic clasts). Welding degree systematically decreases upwards.
	Moderately welded lapilli tuff	Gruvevei Ignimbrite	Gr-Ign	Present across east Alnsjo with maximum thickness of ca. 30 m, but largely patchy exposure in moderately hilly to flat-lying terrain.**	Clast to ash rich units displaying occiasional moderate to incipient fiamme, deformed and elongated clasts, rotated clasts, undeformed pumice and glass lapilli, parallel stratification, and normal to inverse grading. Commonly moderately to poorly sorted ash rich matrix and dominantly juvenile lapilli. Clast lithologies suggest felsic to intermediate compositions. Some units have angular to sub-angular lapilli in basal zones.
	Mudstone	Gruvevei Mudstone	Gr-Mst	Occurrence around the margin of the central Alnsjo region with the best exposure in the east, underlying the Gruvevei Basalt, where ca. 100 m long, 2–4 m thick continuous section is exposed.	Stratified to unstratified, black to red mudstone. Black or dark grey regions exhibit planar to wavy lamination, and minor tabular cross-bedding. Black mudstone grades laterally into red. Red mudstone lacks stratification seen in black mudstone. Possible volcaniclastic interbeds are also present with occasional outsized scoraceous lapilli.
	Ash tuff	Kapteinsmyra Tuff*	Km-Ign	One ca. 3 m thick exposure in the south-central section of the field area. Overlies the Gruvevei Mudstone.**	Thin-stratified lapilli tuff with a thin (ca. 5 cm) marginallly peperitic contact with the underlying mudstone. Planar to wavy stratification is defined by variations in the ash-size fraction and in lapilli abundance. Lapilli is ca. <3 cm, slightly vesciualr, and rounded to slightly elongate.
	Basaltic lava	Gruvevei Basalt	Gr-Ba	Substantial and relatively continuous exposure along the east-central region, with thickness of 16–18 m. Succession repeated due to offset along a small normal fault.	Basaltic lava with a vesicular and peperitic basal zone, dense slightly porphyritic middle region, and rubbly to scoriaceous flow top. Vesicles in the basal zone commonly infilled with mudstone (syn-depositional filling).

Table 1 (continued): Summary of lithostratigraphic units, eruptive and depositional interpretations, and development of overall rift activity.

Phase	Lithology	Units	Unit Abrv.	Spatial distribution	Description
Phase 3	Mudstone	Storhaug Mudstone	St-Mst	Present across the central region of Alnsjo multitude small exposures. Thickness and features found to be very consistent, with thickness of 120 m.	Dominantly unstratified black to red mudstone, with minor carbonate nodule beds and very-fine sand interbeds in the lower 3–4m.
Phase 4	Interstratified mudstone, sandstone, and tuff	Upper Storhaug Mudstone	St-Mst	Found at the top of the Storhaug Mudstone everywhere with very consistent thickness of ca. 15 m.	Interbedded mud, silt, and sand beds with upwards increasing volcaniclastic beds. Sedimentary beds display wavy to ripple laminations and occasional subtle tabular cross-stratifcation. Sedimentary bedding is often deoformed by overlying volcaniclastic interbeds (impact structures and rip-ups). Volcaniclastic beds are ash and pumice rich, thin to moderately thick beds (~1 cm to 10 cm).
	Moderately welded to unwelded ignimbrite	Storhaug Ignimbrite	St-Ign	Found only around the middle of Alnsjø and appears to be laterally discontinuous with up to ca. 8–10 m thickness.	Moderately welded to unwelded ignimbrite with peperitic basal zone. White to pink ash rich groundmass with moderately abundant feldspar micro-phenocrysts. Rich in rounded to amoeboidal and elongate lapilli, becoming more commonly rounded upwards. Elongate lapilli typically show common alignment.
	Volcaniclastic conglomerate	Storhaug Conglomerate	St-Cgm	Marking the top of the succession in the middle of the Alnsjø field. Variably overlies the Storhaug ignimbrite and the Storhaug Mudstone. Minimum preserved thickness of 45 m.	Poorly sorted conglomerate beds with common coarse-tail normal grading and aligned clasts (rarely imbricated). Rarely with thin (~1–4 cm) inversely graded base, Occasional sand to pebbly sand and coarse pebble to cobble clast supported beds interspersed. Basal few metres displays possible indications of primary to mixed deposition (ash rich beds, in-situ brecciation, and occasional fiamme-like textures).

* Unit with limited logging, description, and interpretation due to poor exposure, distribution, or preservation.
** Extremely poorly preserved deposit not shown in maps, cross-sections, or stratigraphic logs.

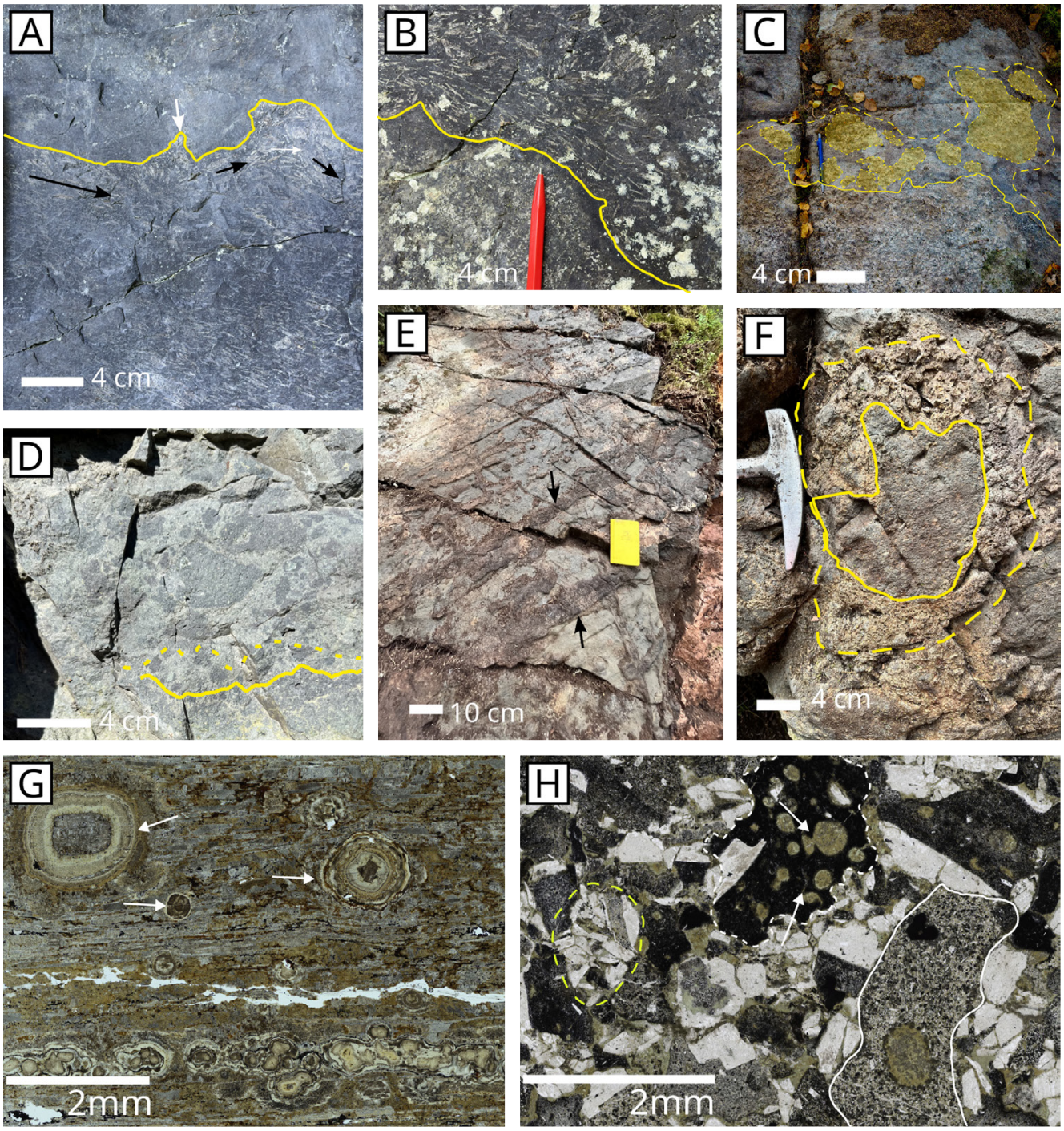

Figure 4: Volcanic features in basaltic units in phase 1. [A] and [B] show aphyric to aphanitic basalt, hosting domains of porphyritic basalt with cuspate to irregular margins (green line), alignment of phenocrysts (especially near boundaries: black arrows), and incipient break-out structure (white arrow). [C] and [D] Syn-depositional brecciation and disaggregation of blocks in the Linderudkollen tuff breccia, with solid lines indicating approximate edge of relatively coherent domains and dotted lines indicating disaggregation boundaries. Clasts in [C] (yellow shaded areas) show irregular/cuspate margins indicative of plastic behaviour during disaggregation. [E] Marginally scoriaceous lenses and bedding (arrows), basaltic clasts, and fine-grained groundmass in the Linderudkollen tuff breccia. [F] Clast interpreted as spatter-bomb in the upper Linderudkollen tuff breccia with a dense core (solid line) surrounded by a marginally vesiculated rind (dashed line). [G] photomicrograph (PPL) of a banded accretionary lapilli tuff inclusion from lower Kringlefjell basalt showing both phenocrysts cored and un-cored accretionary lapilli (white arrows). [H] Photomicrograph of basaltic tuff breccia (PPL) groundmass highlighting angular phenocryst and glass fragments (yellow outline) and two distinct clast types (dashed and solid white outlines) with variable vesicularity, groundmass crystallinity, and clast shapes (blocky vs irregular margins).

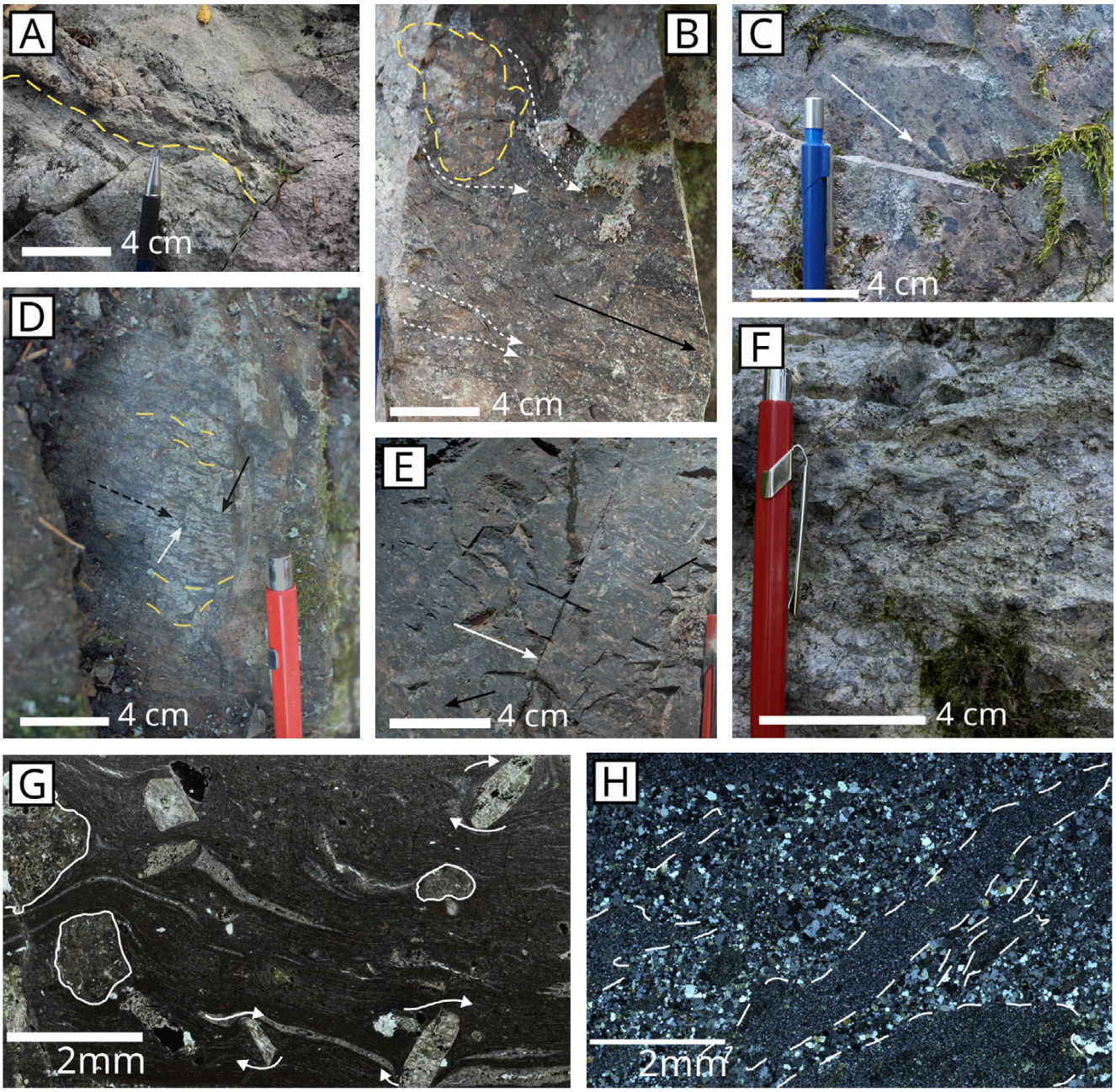

Figure 5: Features of silicic ignimbrites in phase 2. [A]–[C] Basal, middle, and upper zones of the Linderudkollen Ignimbrite showing the textural development from heavily to moderately welded. Dashed yellow line in [A] marks lower contact with Linderudkollen tuff breccia whilst the black dashed line demarcates a small syenitic dike (associated with larger syenitic intrusive complex). Black arrows in [B] and [C] show general stratification orientation whilst white dashed arrows in [B] show wrapping and folding of flow bands around clasts (dashed outline). [A], [B] Dense groundmass, strongly elongate fiamme (black arrows), and aligned phenocrysts (white arrows) indicative of pyroclastic origins and high-degree welding in the lower [D] and middle [E] Svartkulp Ignimbrite. [F] Angular to sub-rounded clasts and minor fiamme in the lower Gruvevei Ignimbrite. [G] Photomicrograph (PPL) of flow banding, rotated phenocrysts (arrows indicate rotations direction), and fine crystalline clasts (white outlines) the Svartkulp lava-like ignimrbite of phase 2. Crystalline clasts are interpreted as cognate inclusions from the crsytallising magma reservoir. [G] Photomicrograph (XPL) of fiamme (white outlines) and groundmass in a completely devitrified densely to moderately welded ignimbrite (Kringlefjell ignimbrite). Fiamme are invariably very small and lack any phenocrysts.

Figure 6: Volcanic and sedimentary features of upper phase 2. [A] Ash-rich beds (dashed black lines) and minor fiamme (dashed yellow outlines) in the uppermost Gruvevei Ignimbrite. [B] Volcaniclastic interbeds and sedimentary stratification in the Gruvevei Mudstone. Dashed lines in [B] mark a volcanic ash layer (possibly reworked). White, black, and red arrows indicate subtle wavy to ripple stratification, tabular cross-stratification, and inferred post-depositional slumping features respectively. [C] Undulating boundary between the Gruvevei Mudstone (below dashed line) and overlying Gruvevei Basalt. [D] Hand-sample of peperite from the basal Gruvevei Basalt showing flow textures within the mudstone (black arrow), mudstone filled vesicles in the basalt clasts (red arrow), and brittle fracturing of vesicles in a basalt clast (dashed circle). [E] Reworked volcaniclastic clasts (black arrows), rare volcanic laminations (dashed lines), and minor brecciation in the lowermost Storhaug Mudstone directly overlying the Gruvevei Basalt. [F] Fine grained, diffuse stratified upper portion of the Gruvevei Basalt with marginally scoriaceous clasts (white arrows) and slight elongation of some large clasts (dashed outline).

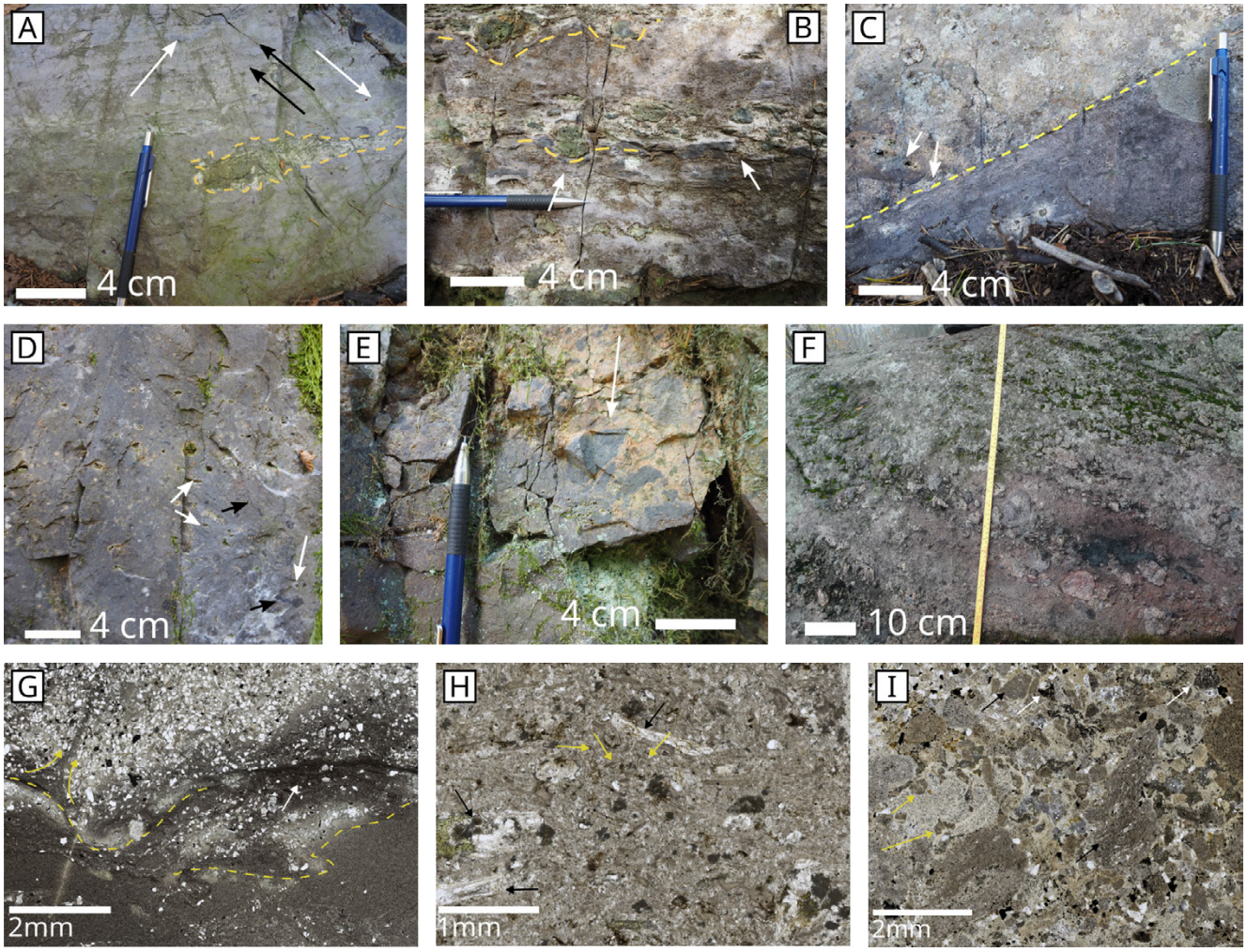

Figure 7: Sedimentary and volcanic features of phase 4. [A] Reworked ash and mudstone zones showing soft sediment deformation (white arrows), volcaniclastic lenses (dashed outline), and sandy interbeds (black arrows). Repeated subtle upwards fining sequences (from ash or reworked ash to fine mudstone) are observed in these outcrops. [B] An example of the mixed volcano-sedimentary portion of the upper Storhaug Mudstone showing bomb-sags (dashed lines) and associated soft-sediment deformation (arrows). [C], [D] Basal contact (dashed line) and middle portion of the Storhaug Ignimbrite respectively. White arrows in [C] show subtle development of peperite indicated by inclusions of mudstone (one with internal vesiculation) in the basal zone. [D] Ash-rich, diffuse-stratified moderately-welded middle portion with stratification defined by elongate vesicles (white arrows) and fine fiamme (black arrows). [E] Brecciation texture (arrow) in the lower Storhaug Conglomerate interpreted as evidence for mixed volcanic and sedimentary activity. [F]An example of a typical bed in the the Storhaug Conglomerate with poor sorting and planar bedding, and dominated by silicic volcanic clasts. [G]–[I] Thin section photomicrographs (all in ppl) of textures in volcanic and volcanogenic units of the upper succession. [G]Interaction between mudstone (dark region in lower half) and volcanic tephra inducing soft sediment deformation (yellow lines and arrows) and mixing of fine mud flakes (white arrow) with the tephra. Yellow arrows indicate a mud injection (i.e. micro-flame structure) into the tephra. [H] Moderately welded ignimbrite (Storhaug ignimbrite) rich in ash fragments (yelllow arrows, including rare y-shaped varieties), and with some altered, crudely alligned phenocryts (black arrows). [I] Groundmass components of a volcanogenic bed from the Storhaug conglomerate highlighting spherulitic devitrification in clasts (yellow arrows), ignimrbite clasts with subtle flow banding (black arrows), and fine mafic clasts (white arrows).

tuff-breccia units allude to changes in eruption dynamics (e.g. phreatomagmatic activity or increased ascent and decompression rates), and/or changes in the magma characteristics (e.g. composition, crystallinity, or volatile content). Previous workers suggested these deposits were the product of local reworking [i.e. were sedimentary deposits: Naterstad 1978] but the poor sorting, irregular, ameoboid clast shapes, and dis-saggregation features rule out a sedimentary origin [e.g. Ross and White 2005]. Furthermore, although ash-rich and with dominantly poorly vesicular clasts, the scarcity of angular ash and lapilli suggest phreatomagmatism was not an important driver [Zimanowski et al. 2015]. Instead, increased viscosity (driven by high crystallinity, cooling, and loss of volatiles) may have lead to development of dense conduit plugs [Lin-

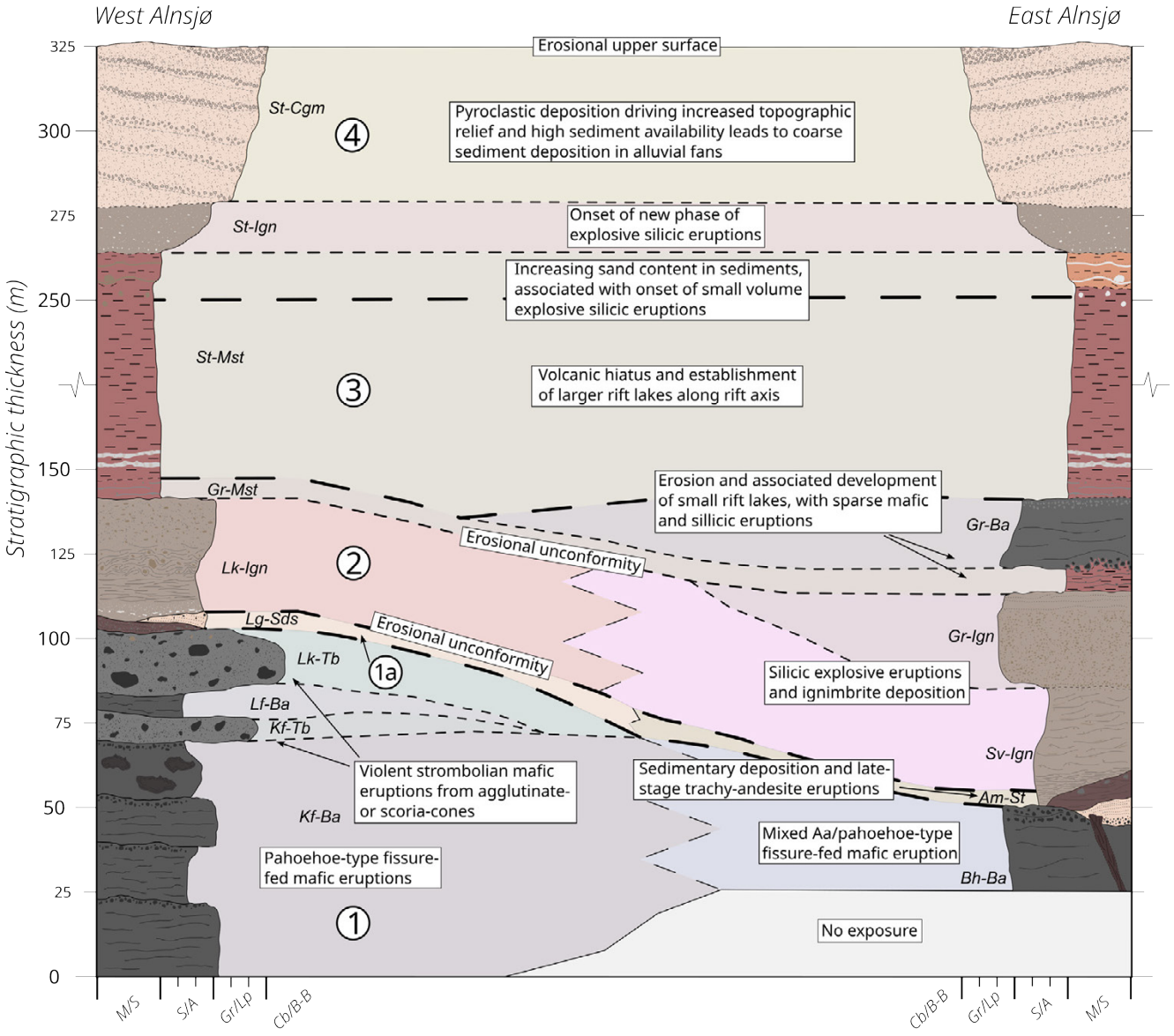

Figure 8: Summarised stratigraphic logs for the west and east of the Alnsjø succession showing interpreted phase boundaries (thick dashed lines; numbers in left half of figure denote phase) and unit boundaries (thin dashed lines). Correlation polygons and abbreviated unit names are the same as those in Figure 2. M/S - mud/silt; S/A - sand/ash; Gr/Lp - gravel/lapilli; Cb/B-B - cobble/block-bomb

doo et al. 2017] or lava domes [Branney and Acocella 2015], hindering magmatic degassing and resulting in Vulcanian to Strombolian style eruptions [e.g. Formenti et al. 2003; Calvari et al. 2012] or lava-dome collapse with block and ash flows and clast comminution [Branney and Kokelaar 2002; Branney and Acocella 2015]. Dominant clast populations in these units (1: porphyritic, dense, with sparse angular clasts; 2: poorly to moderately vesicular, slightly porphyritic, with no angular clasts) represent components derived from a relatively degassed partially-cooled plug or dome, and a comparatively volatile-saturated magma from a deeper reservoir respectively.

5.1.3 *Phase 1a*

Phase 1a is represented by a few poorly preserved volcanic and sedimentary deposits and unconformable contacts with the overlying ignimbrites (Phase 2). The phase comprises fine to coarse grained sediments, (conglomerate, sandstone, and subordinate silt), a trachy-andesite ash-tuff (Alnsjø Tuff), and a pyroclastic trachy-andsite (rhomb-porphyry) dike. Sedimentary deposition preceded emplacement of the rhomb-porphyry dike (indicated by cross-cutting) and although the exact relationship between sedimentary units is obscured by lack of exposure and erosion, the combination is indicative of alluvial to fluvial sedimentation. Dike characteristics such as an ash-rich margin, clastic internal textures, and host-rock brecciation evidence shallow emplacement [Lefebvre et al. 2012; Re et al. 2016], and as such this is interpreted as an eruption-feeding fissure-conduit. The Alnsjø Tuff evidences moderately explosive trachy-andesite eruptions at this time but we have found no clear link to the rhomb-porphyry dike.

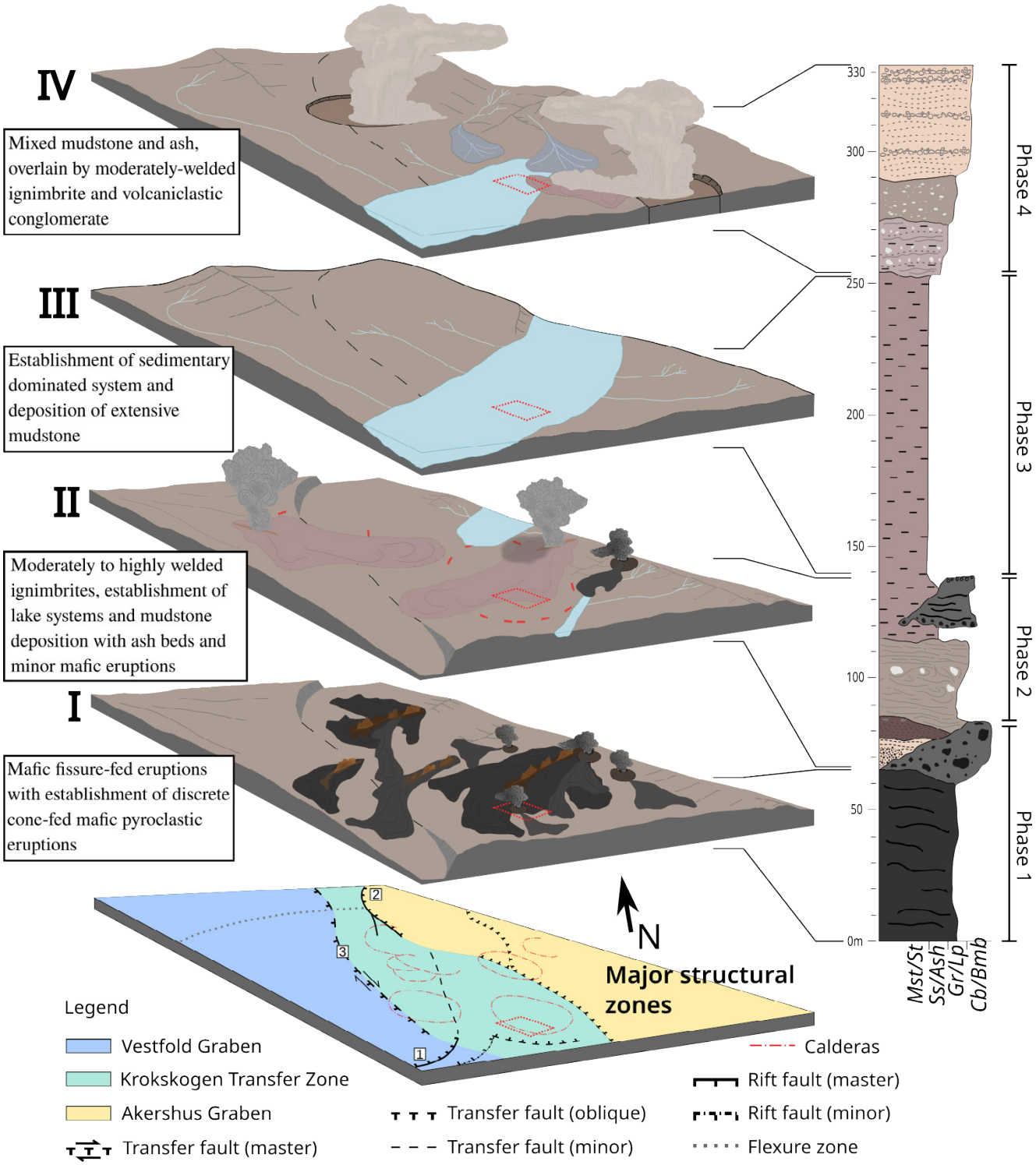

Figure 9: Schematic palaeo-environmental evolution of the sequence preserved in the Alnsjø succession. The area shown in I–IV represents the Krokskogen transfer zone and is the same region as shown in Figure 1B. The dotted red box highlights the approximate location of the Alnsjø region. Faults number 1, 2, and 3 are the Oslofjord master fault, the Randsfjorden-Hunnselv master fault, and the Krokkleiva-Kjaglidalen transfer fault respectively.

Regardless, the unconformable contacts with overlying silicic ignimbrites illustrate a period of erosion following these trachy-andesite eruptions, possibly in relation to period of thermal uplift related to magmatic recharge [e.g. Le Mével et al. 2016; Andersen et al. 2017].

5.1.4 *Phase 2*

Phase 2, comprising silicic ignimbrites, lacustrine mudstone, and a small volume basaltic lava, illustrates a marked changes in both volcanic and sedimentary conditions. Volcanism re-initiated with high-temperature silicic eruptions, producing densely welded ignimbrites (Svartkulp and Linderudkollen ignimbrites) that unconformably overlie the deposits of Phase 1 and 1a. Although it is unclear how some poorly preserved ignimbrites fit into the stratigraphy, there is an apparent rapid evolution from densely welded and lava-like [i.e. Snake-river-type: Branney et al. 2007] to moderately welded and unwelded ignimbrites, with increasing juvenile and lithic clast proportions up-section. Densely welded, lava-like and rheomorphic ignimbrites are interpreted by several authors [e.g. Branney et al. 1992; Branney et al. 2007; Andrews and Branney 2010; Brown and Bell 2013; Lenhardt et al. 2017] as the deposits of highly explosive eruptions emanating from fissures or wide conduits with relatively low eruption columns [perhaps indicated by thin or absent air-fall deposits: Branney and Kokelaar 2002], possibly in conjunction with anomalously high eruptive temperatures [e.g. Andrews and Branney 2010] whereas moderately welded to unwelded ignimbrites are typical of sub-Plinian to Plinian eruptions [Cioni et al. 2015], wherein higher eruption columns and greater fragmentation promote enhanced cooling of pyroclastic material [Branney and Kokelaar 1992]. Densely welded ignimbrites in the Oslo Rift may have utilised preexisting basaltic and trachy-andesite fissures, with later eruptions emanating from volcanic centres or complexes with discrete conduits. Fine-grained sediments (dominantly mudstone) were deposited contemporaneously with basaltic and silicic units during waning volcanism. Sandy inter-beds, fining-up sequences, asymmetrical ripples and tabular cross-bedding, and thin volcaniclastic beds illustrate fluctuating depositional energy and repeated, small-volume volcanic inputs, whilst peperitic basal zones in volcanic units (Kapteinsmyra Ignimbrite and Gruvevei Basalt: Figure 6C, 6D) demonstrate contemporaneity of sedimentary and volcanic deposition [e.g. Jerram and Stollhofen 2002; Waichel et al. 2007]. Lacustrine deltaic environments are typified by generally low but fluctuating depositional energy conditions [Tye and Coleman 1989], and rapid delta growth has been observed as a direct consequence of ash-rich eruptions [Beigt et al. 2019]. The moderately welded to unwelded ignimbrites in the second half of phase 2 were likely drivers of a change in sedimentation, coincident with increasing sedimentary stability due to waning volcanism. As mudstone deposition is continuous in places, the final eruptions of this phase must have been small and the deposits areally-restricted.

5.1.5 *Phase 3*

Phase 3 comprises purely sedimentary portion of the Storhaug Mudstone (i.e. excluding the upper 10–15 m of inter-bedded mudstone, sandy mudstone, and primary volcaniclastics), interpreted as continued development of lacustrine environments. Erosion of underlying silicic units apparently accompanied or preceded deposition, indicated by contacts with both phase 1 and 2 units. Nodular carbonates in the lower 2–5 m represent low-stands initially fluctuating water levels [e.g. Stanistreet et al. 2020], whilst upwards decreasing abundance of stratification is indicative of lake expansion (deeper, calmer waters) and cessation of volcanism, at least in the central rift.

5.1.6 *Phase 4*

Deposits in phase 4 signal renewal of volcanism and rapid changes in the sedimentary system. Scattered, sparse pumice clasts enclosed in unstratified mudstone evidence volcanic renewal, although they are likely secondary volcaniclastics within the schema of Di Capua et al. [2022]. Upwards increasing primary and secondary [*sensu* Di Capua et al. 2022] volcaniclastic inter-beds characterise the upper ca. 10 m of the mudstone, with numerous soft-sediment deformation indicators (bomb-sags, rip-down/rip-up, and flame structures: Figure 7A, 7B, and 7G). Sandy inter-beds consistently overly volcaniclastic beds and fine upwards to mud or sandy mud (i.e. typical background sedimentation) reflecting periodic availability of loosely-compacted ash produced by small volume eruptions rather than a systematic change in sediment transport energy. Rip-up clasts and bomb-sags further indicate that volcanic deposition occurred as both ash-flows and air-fall into shallow water or semi-dry lake shores. Stratigraphic evidence of soft-sediment deformation would less prominent in a deep-water setting due to rapid dissipation and deceleration of small volume ash flows and bombs. The stratigraphic characteristics are consistent with small cinder-cone type edifices [Valentine et al. 2005] which have been shown as a early feature of new volcanic phases [Dóniz-Páez 2015]. In combination with the overlying Storhaug Ignimbrite, these deposits signal initiation of a new volcanic phase characterised by increasingly frequent small-volume eruptions, giving way to comparatively substantial pyroclastic eruptions that produced moderately welded ignimbrites.

In the absence of clear evidence for significant and sudden changes in environmental conditions, alluvial fan development (i.e. the Storhaug Conglomerate) is viewed as indicating a regular supply of partially consolidated (i.e. unwelded to moderately welded) pyroclastic material [e.g. Palmer and Neall 1991; Palmer et al. 1993; Zanchetta et al. 2004]. The dominance of volcaniclastic components, bedding orientation (20-30 degrees), lithofacies (see Supplementary Material 1) and stratification in the Storhaug Conglomerate are analogous to volcaniclastic-rich alluvial fans described in southern Campania [Zanchetta et al. 2004], wherein alluvial fan development is strongly coupled to antecedent ignimbrite deposition suggesting ongoing volcanic activity in the central rift. The final phase of the Alnsjø succession thus records volcanic renewal in the Oslo Rift, initiated with small-volume eruptions that affected transient, but increasingly common perturbations to background sedimentation, followed by the onset of sub-Plinian to Plinian scale eruptions that induced a more substantial and persistent change in the sedimentary system.

5.2 Timing

The Alnsjø succession has been viewed as the youngest deposits present in the Oslo Rift. However, previous researchers indicate a common association between the last significant basaltic phase (denoted as B3) and the trachy-andesite unit RP13 [Oftedahl 1978a], wherein RP13 invariably overlies B3. Naterstad Naterstad [1978] suggested the rhomb-porphyry in the east of Alnsjø occupied a high stratigraphic position (RP13) within the romb-porphyry lava series of the central rift. Rhomb-porphyries in the Oslo Rift are numbered based on unique phenocryst assemblages [summary in Oftedahl 1978b], therefore, although reclassified as a shallow lava conduit, the relative position within the lava series is likely still valid. Following this association, the cross-cutting relationship between RP13-dike and Breisjøhogdene basalt in the east illustrates that the lower basaltic units are related to the B3 phase and are older than previously thought. Therefore, we interpret the Svartkulp and Linderudkollen ignimbrites as recording the onset of major silicic eruptions in the central rift.

5.3 Intra- or extra-caldera deposition

Silicic volcanic successions and deposits throughout the Oslo Rift have commonly been perceived as late-stage intra-caldera infill [Sæther 1946; Naterstad 1978; Larsen et al. 2008], evidenced by presence within approximately circular to elliptical structures with apparent juxtaposition of older and younger units across the boundaries of these structures. However, although the Alnsjø succession is located very close to a proposed caldera ring-fault with large inferred subsidence magnitude [~1–2 km subsidence: Sæther 1946; Sørensen 1975; Naterstad 1978; Oftedahl 1978a], stratigraphic evidence of caldera-collapse concomitant with the volcano-sedimentary succession is absent. Commonly, lower units of a caldera-fill succession or upper portions of caldera-forming ignimbrites will contain mega- or meso-breccias, especially adjacent to the caldera ring fault, related to collapse of newly-formed, unstable caldera walls [Lipman 1976; Moore and Kokelaar 1998; Brown and Branney 2003]. Furthermore, syn- or post-collapse ignimbrites would reasonably be expected to show evidence of ponding or draping relationships with a caldera fault-scarps, or on-lapping relationships with collapse breccias [Moore and Kokelaar 1998; Lipman et al. 2015]. Regarding sedimentary caldera infill, fining-up sequences are more typical of post-collapse deposition due to initially unstable caldera walls feeding coarse-grained material to the system, and a general increase in stabilisation with time leading to slower sedimentation rates [Branney and Acocella 2015]. These features are all absent in the Alnsjø succession. Moreover, evidence for caldera collapse concomitant with preserved deposits is lacking or not sufficiently documented in all but one area [Drammen: Andersen 2024] in the Oslo Rift. Apparent cone-sheet intrusions slightly south-west to south-east of the arcuate boundary of the Alnsjø do imply later caldera collapse but the preserved succession represents a subsided caldera block, wherein the small-scale faulting and broad deformation reflect piecemeal collapse [e.g. Moore and Kokelaar 1998] and flexural subsidence [e.g. Walker 1984] respectively.

5.4 Silicic volcanism across the Oslo Rift

Silicic volcanic units across the Oslo Rift have commonly been mis-interpreted and under-represented in previous studies, and it is only recently that the extent of these units has been recognised [e.g. Lutro and Nordgulen 2008]. Invariably, the ignimbrites have been treated as intra-caldera deposits, although the presented for this evidence is limited and essentially consists of the inferred presence of ring-dikes and the juxtaposition of units from disparate stratigraphic levels. However, the Alnsjø succession shows no evidence of caldera collapse, and consistent stratigraphic dips in all but the uppermost conglomerate indicates deposition in roughly flat-lying regions (assuming approximately horizontal deposition of lacustrine sediments). Densely welded ignimbrites lacking evidence for caldera collapse may be influenced by local tectonic structures [Navarrete et al. 2020; Drake et al. 2022] but may also be medial to distal sections of caldera forming ignimbrites. Cursory observations to the north-west [e.g. the Bærum, Oppkuven, or Kampen calderas: Lutro and Nordgulen 2008; Corfu and Larsen 2020] highlights the presence of densely welded, crystal-rich ignimbrites [mapped as rhyolites and ignimbrites in Lutro and Nordgulen 2008] that are texturally comparable to the Svartkulp and Linderudkollen ignimbrites. These units were long misinterpreted as varied porphyritic granites and syenites [e.g. Olerud 2002] or as intrusive breccias and felsites [e.g. Oftedahl 1946], which led to suggestions that no evidence for ignimbrites existed in this region (the Krokskogen Plateau) of the Oslo Rift [Larsen et al. 2008]. No recent descriptive or stratigraphic work has been undertaken in these areas, but the map of Lutro and Nordgulen Lutro and Nordgulen [2008] shows a similar succession to phase 1–2 of Alnsjø, with basalt(s), overlain by relatively late-stage rhomb-porphyry lava(s) (regionally labelled rhomb-porphyry 11 (RP11); wherein the latest flows are typically numbered RP13-15), overlain by a rhyolitic unit(s). In addition, recent work in a caldera to the south [Andersen 2024] illustrates a similar evolution in the silicic phase (first producing densely welded ignimbrites, with a rapid shift to moderately welded and unwelded ignimbrites) but the succession lacks most of the basaltic, trachy-andesite, and sedimentary units preserved in Alnsjø. Conversely, the basal densely welded ignimbrite observed there is substantially thicker (ca. 300 m) and displays some evidence (e.g. ring-fault bounded coarse breccias) supporting concomitant caldera collapse [Andersen 2024]. The combination of significantly thicker individual ignimbrites and evidence of caldera collapse suggests these were the primary eruption centres active during the early silicic phase but the current lack of detailed stratigraphic, lithofacies, geochemical, and geochronological data from this phase precludes verification of this. Deposition of thick ignimbrites may have hindered sedimentary deposition in proximal regions due to disturbance or complete destruction of the palaeoenvironment and sedimentary pathways and increased post-eruption topography [Manville and Wilson 2004; Manville et al. 2009], with sediments rapidly draining towards topographically lower rift axis settings [Ebinghaus et al. 2014] where silicic volcanic units were comparatively thin medial to distal deposits from other centres. Rift axis depocentres similar

to the Gregory Rift (Southern East African Rift), which contain rift valley lakes [Scoon 2018], on- and off-axis central volcanic complexes and calderas [Bosworth 1987; Scoon 2018], and cinder-cones [Martin-Jones et al. 2019], is in better agreement with the stratigraphic evidence than prior suggestions of intra-caldera deposition. The diverse lithostratigraphy of the Alnsjø succession is somewhat unusual in the Oslo Rift, with no similar examples known. The primary cause is substantial rift-wide glacial erosion, with many areas now dominated by intrusive rocks or covered by sea (the Oslo Fjord; Figure 1A). Consequently, the Alnsjø succession likely represents the only type locality, and a valuable reference sequence for late-stage volcano-sedimentary evolution in the Oslo Rift. Additionally, the potential for erosion and modification of such deposits means that their occurrence within the rock record could be somewhat underrepresented, compared to a similar modern day setting.

5.5 Episodic volcanism and rapid source variations

Although the relationship between some units is obscured by lack of exposure and erosion the variability observed in the Alnsjø succession illustrates rapid evolution or variations in magmatic source(s) that appears to be characteristic of early silicic volcanism in the Oslo Rift. Many other silicic volcanic provinces are characterised by broadly uniform styles of ignimbrite. These can be typified by high-grade ignimbrites [e.g. Andrews et al. 2007] or by low- to moderate-grades [e.g. Brown et al. 2003] of ignimbrite. The British Paleogene Igneous Province (BPIP) for example illustrates a contrasting setting wherein ignimbrites display evidence of rapid and frequent variations between these endmember styles [Brown et al. 2024]. Although the development of silicic systems in the BPIP was often in the latter stages such as on the isle of Skye, early caldera development of this province also occurs [Troll et al. 2019]. Similarly, development of silicic ignimbrite eruptions in the Main Ethiopian rift (northern east African rift) occurred both in the early stages of rift initiation (intercalated with basalts) and in later stages [Wolfenden et al. 2004]. In contrast, Ignimbrites in Alnsjø (and more broadly, across the Oslo Rift) appear to illustrate a dominant evolution in style from densely welded ignimbrites at the onset, to moderately welded and unwelded ignimbrites in following eruptions, this pattern being repeated across different eruptive centres, but only occurring within the later stages of the Oslo Rift volcanic system. The accretionary-lapilli ash rip-up in the lowermost basalt represents the earliest known silicic volcanism and was likely triggered by the arrival of basaltic composition magmas that subsequently fed the overlying eruptions but also implies that silicic magma reservoirs were already present. Additionally, these basaltic magmas may have provided the heat required to generate the high-temperature snake-river-type silicic eruptions that comprise the onset of the phase 2 sequence from pre-existing silicic reservoirs. However, whilst rare silicic clasts are present in the basaltic tuff breccia unit, densely welded ignimbrites are devoid of mafic clasts, which might be expected from an episode of mafic recharge [e.g. Liszewska et al. 2018]. Mafic phenocrysts may be present in these rocks but pervasive alteration of phenocryst compositions throughout the Oslo Rift generally rules out confident assessment of such features. Younger moderately welded and unwelded ignimbrites in Alnsjø do contain minor mafic clasts (especially in the Storhaug Ignimbrite) and may relate to separate magmatic sources that had more interaction with mafic magma recharge, or alternatively may signal significant emptying of silicic reservoirs in the early eruptions creating space for mafic recharge. The early densely welded ignimbrites may instead represent evacuations of rapidly emplaced, shallow, hot magma reservoirs [e.g. Castro et al. 2013; Rhodes et al. 2021; Repstock et al. 2022]. Evidence for shallow emplacement of overlapping and cross-cutting silicic reservoirs is commonplace in the Oslo Rift (e.g. the cross-cutting syenite, granite, and nordmakite bodies surrounding Alnsjø: Figure 1). The long volcanic hiatus represented by phase 3 likely relates to somewhat complete emptying of available melt from magma reservoirs during the phase 2 eruptions, resulting in cooling and rheological lock-up of remaining magmatic mush [e.g. Rhodes et al. 2021], and emplacement of new silicic reservoirs. Eruptions in phase 4 contain mafic material, and whilst no direct evidence for basaltic eruptions at this stage is present in Alnsjø, they are documented elsewhere in rift at the same stratigraphic level [e.g. Larsen et al. 2008]. Nonetheless, these were deeper and/or cooler reservoirs such that the onset of phase 4 volcanism was typified by lower temperature, comparatively pumice- and ash-rich ignimbrites with higher lithic contents. The Alnsjø succession thus illustrates episodic and variable silicic volcanism, likely driven by a combination of large-volume, shallow reservoirs and rapid emplacement of distinct silicic magma batches. This likely required a complex transcrustal magmatic plumbing system and periodic basaltic re-heating, wherein the depth and emplacement timescales of reservoirs may have been the primary drivers of eruption style. Initial silicic volcanism in the Oslo Rift displays similar lithofacies and stratigraphic characteristics to Snake-River-type deposits but notably, is characterised by compositionally tri-modal volcanic products and rapid evolution in the intensity of welding in ignimbrites, signalling rapid changes in source region and/or magma reservoir and eruption conditions.

6 Conclusions

We present a revised geological map and the first comprehensive litho-stratigraphic reconstruction of the volcano-sedimentary evolution in the central Oslo Rift. Stratigraphic relationships indicate the succession is older than previously thought and likely records some of the earliest silicic volcanism in the Oslo Rift. Four key phases of volcanic and sedimentary deposition are distinguished, separated by erosional hiatuses and/or clear changes in depositional conditions. The succession records late-stage basaltic lava flows, signalling, a transition towards pyroclastic (e.g. cinder-cone) edifices, and final phases of trachy-andesite volcanism in the Oslo Rift, with the basaltic pyroclastic deposits being the first of their kind reported in the Oslo Rift. Partially preserved sedimentary and intermediate-composition volcanic units overlying the basaltic units represent the onset of a period dominantly characterised by sedimentation and erosion, with minor volcanism. Several, variably preserved rheomorphic and lava-like to moderately-

welded ignimbrites record some of the earliest phases of dominantly silicic magmatism in the central to northern rift, but are evidently not the first eruptions of evolved compositions given the banded-rhyolite inclusion in the lowermost basalt in the west of the study area. Lacustrine to and minor fluvial deposits overlying these ignimbrites record a period of volcanic quiescence and development of rift lakes contemporaneously with waning volcanic activity. Mudstone with volcaniclastic inter-beds, a moderately welded ignimbrite, and coarse sediment deposition illustrate both volcanic renewal and a change in the sedimentary deposition driven by increased local topography and sediment availability. Contrary to conclusions of prior research, we find no evidence to suggest this succession records a caldera-collapse episode and subsequent infilling. However, tentative correlation with an area in the west of the Krokskogen area, where a similar sequence of basalt, trachy-andesite, and rheomorphic to lava-like ignimbrite exists suggests eruptive-centres, and therefore signs of any caldera-collapse for the phase 2 ignimbrites might be further west. Early silicic eruptions lack evidence for mafic recharge as an eruption trigger whereas later ignimbrites do. Early rheomorphic to lava-like ignimbrites were likely the product of large, shallow, and rapidly-emplaced silicic reservoirs undergoing near-complete emptying of available melt. Rapid progression to moderately and unwelded ignimbrites in subsequent eruptions indicates modification of source reservoirs following a large eruption, or rapid switching between reservoirs. Compared to other global examples of modern and ancient systems showing similar juxtaposition of lithofacies types, the Alnsjø succession shows some similarity to Snake-River type deposits, but notably differs in its compositionally tri-modal volcanic products and rapid evolution from high- to low-grade ignimbrites. This evolution appears to be consistently shown in other silicic eruptive centres of the Oslo Rift.

Author Contributions

Jack W. Whattam conducted the geological mapping, collection of field data, initial conceptualisation of ideas and figures as part of his PhD studies. Ivar Midtkandal, Dougal A. Jerram, Sara Callegaro, and Henrik H. Svensen contributed to data interpretations, discussing concepts and implications, and manuscript review and figure editing, as well as in PhD supervisory roles.

Acknowledgements

J. W. would like to thank John Millett for invaluable discussions that improved the interpretation of certain magmatic features. S.C. acknowledges support from the Research Council of Norway (Young Research Talents, grant 301096). D. A. Jerram is partly funded through the Research Council of Norway's 'Beyond Elasticity' project (grant 334654). The two anonymous reviewers are thanked for their thoughtful and helpful comments that greatly improved the manuscript. Fabian Wadsworth is thanked for editorial support and feedback.

Data Availability

Supplementary Material comprising detailed descriptions and interpretations of the geological succession is available alongside the online version of this article.

Copyright Notice

References

Alberti, M. and M. Zanieri (2023). *qProf*. URL: https://github.com/mauroalberti/qProf.

Andersen, G. L. (2024). "The explosive volcanism of the Oslo Rift - insights from the ignimbrites of the Drammen Caldera". URI :http://hdl.handle.net/10852/113067. Master's thesis. Universitet i Oslo.

Andersen, N. L., B. S. Singer, B. R. Jicha, B. L. Beard, C. M. Johnson, and J. M. Licciardi (2017). "Pleistocene to Holocene Growth of a Large Upper Crustal Rhyolitic Magma Reservoir beneath the Active Laguna del Maule Volcanic Field, Central Chile". *Journal of Petrology* 58(1), pages 85–114. DOI: 10.1093/petrology/egx006.

Andersen, T., A. Saeed, R. H. Gabrielsen, and S. Olaussen (2011). "Provenance characteristics of the Brumunddal sandstone in the Oslo Rift derived from U-Pb, Lu-Hf and trace element analyses of detrital zircons by laser ablation ICMPS". *Norwegian Journal of Geology* 91(1–2), pages 1–18.

Andrews, G. D. M. and M. J. Branney (2010). "Emplacement and rheomorphic deformation of a large, lava-like rhyolitic ignimbrite: Grey's Landing, southern Idaho". *Geological Society of America Bulletin* 123(3–4), pages 725–743. DOI: 10.1130/b30167.1.

Andrews, G. D. M., M. J. Branney, B. Bonnichsen, and M. McCurry (2007). "Rhyolitic ignimbrites in the Rogerson Graben, southern Snake River Plain volcanic province: volcanic stratigraphy, eruption history and basin evolution". *Bulletin of Volcanology* 70(3), pages 269–291. DOI: 10.1007/s00445-007-0139-0.

Barreto, C. J. S., E. F. de Lima, C. M. Scherer, and L. d. M. M. Rossetti (2014). "Lithofacies analysis of basic lava flows of the Paraná igneous province in the south hinge of Torres Syncline, Southern Brazil". *Journal of Volcanology and Geothermal Research* 285, pages 81–99. DOI: 10.1016/j.jvolgeores.2014.08.008.

Beigt, D., G. Villarosa, V. Outes, E. A. Gómez, and G. Toyos (2019). "Remobilized Cordón Caulle 2011 tephra deposits in north-Patagonian watersheds: Resedimentation at deltaic environments and its implications". *Geomorphology* 341, pages 140–152. DOI: 10.1016/j.geomorph.2019.05.023.

Benton, M. J. (2018). "Hyperthermal-driven mass extinctions: killing models during the Permian–Triassic mass ex-

tinction". *Philosophical Transactions of the Royal Society A: Mathematical, Physical and Engineering Sciences* 376(2130), page 20170076. DOI: 10.1098/rsta.2017.0076.

Bosworth, W. (1987). "Off-axis volcanism in the Gregory rift, east Africa: Implications for models of continental rifting". *Geology* 15(5), page 397. DOI: 10.1130/0091-7613(1987)15<397:ovitgr>2.0.co;2.

Branney, M. J. (1995). "Downsag and extension at calderas: new perspectives on collapse geometries from ice-melt, mining, and volcanic subsidence". *Bulletin of Volcanology* 57(5), pages 303–318. DOI: 10.1007/bf00301290.

Branney, M. J. and V. Acocella (2015). "Calderas". *The Encyclopedia of Volcanoes (Second Edition)*. Edited by H. Sigurdsson. Academic Press: 2nd ed, pages 299–315. DOI: 10.1016/B978-0-12-385938-9.00016-X.

Branney, M. J., B. Bonnichsen, G. D. M. Andrews, B. Ellis, T. L. Barry, and M. McCurry (2007). "'Snake River (SR)-type' volcanism at the Yellowstone hotspot track: distinctive products from unusual, high-temperature silicic supereruptions". *Bulletin of Volcanology* 70(3), pages 293–314. DOI: 10.1007/s00445-007-0140-7.

Branney, M. J., B. P. Kokelaar, and B. J. McConnell (1992). "The Bad Step Tuff: a lava-like rheomorphic ignimbrite in a calc-alkaline piecemeal caldera, English Lake District". *Bulletin of Volcanology* 54(3), pages 187–199. DOI: 10.1007/bf00278388.

Branney, M. J. and P. Kokelaar (1992). "A reappraisal of ignimbrite emplacement: progressive aggradation and changes from particulate to non-particulate flow during emplacement of high-grade ignimbrite". *Bulletin of Volcanology* 54(6), pages 504–520. DOI: 10.1007/bf00301396.

– (1994). "Volcanotectonic faulting, soft-state deformation, and rheomorphism of tuffs during development of a piecemeal caldera, English Lake District". *Geological Society of America Bulletin* 106(4), pages 507–530. DOI: 10.1130/0016-7606(1994)106<0507:vfssda>2.3.co;2.

– (2002). "Pyroclastic Density Currents and the Sedimentation of Ignimbrites". *Geological Society, London, Memoirs* 27(1). DOI: 10.1144/gsl.mem.2003.027.

Brøgger, W. (1890). "Die Mineralien der Syenitpegmatitgänge der Südnorwegischen Augit- und Nephelinsyenite". *Zeitschrift Für Krystallographie Und Mineralogie* 16(I–XVIII).

Brown, D., A. Quirie, P. Reynolds, and S. Drake (2024). ""Hot and sticky" and "cold and damp" pyroclastic eruptions, and their relationship with topography: valley- and lake-filling ignimbrites, Ardnamurchan, NW Scotland". *Volcanica* 7(2), pages 503–524. DOI: 10.30909/vol.07.02.503524.

Brown, D. J. and B. R. Bell (2013). "The emplacement of a large, chemically zoned, rheomorphic, lava-like ignimbrite: the Sgurr of Eigg Pitchstone, NW Scotland". *Journal of the Geological Society* 170(5), pages 753–767. DOI: 10.1144/jgs2012-147.

Brown, R. J., T. L. Barry, M. J. Branney, M. S. Pringle, and S. E. Bryan (2003). "The Quaternary pyroclastic succession of southeast Tenerife, Canary Islands: explosive eruptions, related caldera subsidence, and sector collapse". *Geological Magazine* 140(3), pages 265–288. DOI: 10.1017/S0016756802007252.

Brown, R. J., S. Blake, T. Thordarson, and S. Self (2014). "Pyroclastic edifices record vigorous lava fountains during the emplacement of a flood basalt flow field, Roza Member, Columbia River Basalt Province, USA". *Geological Society of America Bulletin* 126(7–8), pages 875–891. DOI: 10.1130/b30857.1.

Brown, R. and M. Branney (2004). "Bypassing and diachronous deposition from density currents: Evidence from a giant regressive bed form in the Poris ignimbrite, Tenerife, Canary Islands". *Geology* 32(5), page 445. DOI: 10.1130/g20188.1.

Brown, R. J. and M. J. Branney (2003). "Event-stratigraphy of a caldera-forming ignimbrite eruption on Tenerife: the 273 ka Poris Formation". *Bulletin of Volcanology* 66(5), pages 392–416. DOI: 10.1007/s00445-003-0321-y.

Bryan, S., R. Cas, and J. Martı (1998). "Lithic breccias in intermediate volume phonolitic ignimbrites, Tenerife (Canary Islands): constraints on pyroclastic flow depositional processes". *Journal of Volcanology and Geothermal Research* 81(3–4), pages 269–296. DOI: 10.1016/s0377-0273(98)00004-3.

Bryan, S. E., T. R. Riley, D. A. Jerram, C. J. Stephens, and P. T. Leat (2002). "Silicic volcanism: An undervalued component of large igneous provinces and volcanic rifted margins". *Volcanic Rifted Margins*. Edited by M. A. Menzies, S. L. Klemperer, C. J. Ebinger, and J. Baker. Geological Society of America. ISBN: 9780813723624. DOI: 10.1130/0-8137-2362-0.97.

Burchardt, S. (2008). "New insights into the mechanics of sill emplacement provided by field observations of the Njardvik Sill, Northeast Iceland". *Journal of Volcanology and Geothermal Research* 173(3–4), pages 280–288. DOI: 10.1016/j.jvolgeores.2008.02.009.

Calvari, S., R. Büttner, A. Cristaldi, P. Dellino, F. Giudicepietro, M. Orazi, R. Peluso, L. Spampinato, B. Zimanowski, and E. Boschi (2012). "The 7 September 2008 Vulcanian explosion at Stromboli volcano: Multiparametric characterization of the event and quantification of the ejecta". *Journal of Geophysical Research: Solid Earth* 117(B5). DOI: 10.1029/2011jb009048.

Cassinis, G., C. R. Perotti, and A. Ronchi (2011). "Permian continental basins in the Southern Alps (Italy) and peri-mediterranean correlations". *International Journal of Earth Sciences* 101(1), pages 129–157. DOI: 10.1007/s00531-011-0642-6.

Castro, J. M., C. I. Schipper, S. P. Mueller, A. S. Militzer, A. Amigo, C. S. Parejas, and D. Jacob (2013). "Storage and eruption of near-liquidus rhyolite magma at Cordón Caulle, Chile". *Bulletin of Volcanology* 75(4). DOI: 10.1007/s00445-013-0702-9.

Cioni, R., M. Pistolesi, and M. Rosi (2015). "Plinian and Subplinian Eruptions". *The Encyclopedia of Volcanoes*. Edited by H. Sigurdsson. 2nd edition. Elsevier, pages 519–535. ISBN: 9780123859389. DOI: 10.1016/b978-0-12-385938-9.00029-8.

Corfu, F. and S. Dahlgren (2008). "Perovskite U–Pb ages and the Pb isotopic composition of alkaline volcanism initiating the Permo-Carboniferous Oslo Rift". *Earth and Planetary Science Letters* 265(1–2), pages 256–269. DOI: 10.1016/j.epsl.2007.10.019.

Corfu, F. and B. T. Larsen (2020). "U-Pb systematics in volcanic and plutonic rocks of the Krokskogen area: Resolving a 40 million years long evolution in the Oslo Rift". *Lithos* 376–377, page 105755. DOI: 10.1016/j.lithos.2020.105755.

Czuppon, G., R. Lukács, S. Harangi, P. R. Mason, and T. Ntaflos (2012). "Mixing of crystal mushes and melts in the genesis of the Bogács Ignimbrite suite, northern Hungary: An integrated geochemical investigation of mineral phases and glasses". *Lithos* 148, pages 71–85. DOI: 10.1016/j.lithos.2012.06.009.

Dahlgren, S., F. Corfu, and L. Heaman (1996). "U–Pb time constraints, and Hf and Pb source characteristics of the Larvik plutonic complex, Oslo Paleorift. Geodynamic and geochemical implications for the rift evolution. VM Goldschmidt Conference". *Journal of Conference Abstracts*. Volume 1. Cambridge Publications, page 120.

Di Capua, A., R. De Rosa, G. Kereszturi, E. Le Pera, M. Rosi, and S. F. L. Watt (2022). "Volcanically-derived deposits and sequences: a unified terminological scheme for application in modern and ancient environments". *Geological Society, London, Special Publications* 520(1), pages 11–27. DOI: 10.1144/sp520-2021-201.

DiMichele, W. A., H. W. Pfefferkorn, and R. A. Gastaldo (2001). "Response of Late Carboniferous and Early Permian Plant Communities to Climate Change". *Annual Review of Earth and Planetary Sciences* 29(1), pages 461–487. DOI: 10.1146/annurev.earth.29.1.461.

Dóniz-Páez, J. (2015). "Volcanic geomorphological classification of the cinder cones of Tenerife (Canary Islands, Spain)". *Geomorphology* 228, pages 432–447. DOI: 10.1016/j.geomorph.2014.10.004.

Drake, S. M., D. Brown, A. Beard, P. Kumlertsakul, D. Thompson, C. Bays, I. Millar, and K. Goodenough (2022). "Catastrophic caldera-forming eruptions and climate perturbations: the result of tectonic and magmatic controls on the Paleocene-Eocene Kilchrist Caldera, Isle of Skye, NW Scotland". *Volcanica* 5(2), pages 397–432. DOI: 10.30909/vol.05.02.397432.

Dreher, S. T., J. C. Eichelberger, and J. F. Larsen (2005). "The Petrology and Geochemistry of the Aniakchak Caldera-forming Ignimbrite, Aleutian Arc, Alaska". *Journal of Petrology* 46(9), pages 1747–1768. DOI: 10.1093/petrology/egi032.

Duraiswami, R. A., P. Gadpallu, T. N. Shaikh, and N. Cardin (2014). "Pahoehoe–aa transitions in the lava flow fields of the western Deccan Traps, India-implications for emplacement dynamics, flood basalt architecture and volcanic stratigraphy". *Journal of Asian Earth Sciences* 84, pages 146–166. DOI: 10.1016/j.jseaes.2013.08.025.

Ebbing, J., Y. Afework, O. Olesen, and Ø. Nordgulen (2005). "Is there evidence for magmatic underplating beneath the Oslo Rift?" *Terra Nova* 17(2), pages 129–134. DOI: 10.1111/j.1365-3121.2004.00592.x.

Ebinghaus, A., A. J. Hartley, D. W. Jolley, M. Hole, and J. Millett (2014). "Lava-Sediment Interaction and Drainage-System Development In A Large Igneous Province: Columbia River Flood Basalt Province, Washington State, U.S.A". *Journal of Sedimentary Research* 84(11), pages 1041–1063. DOI: 10.2110/jsr.2014.85.

Formenti, Y., T. H. Druitt, and K. Kelfoun (2003). "Characterisation of the 1997 Vulcanian explosions of Soufri?re Hills Volcano, Montserrat, by video analysis". *Bulletin of Volcanology* 65(8), pages 587–605. DOI: 10.1007/s00445-003-0288-8.

Galland, O., H. de la Cal, J. Mescua, and O. Rabbel (2022). "3-dimensional trapdoor structure of laccolith-induced doming and implications for laccolith emplacement, Pampa Amarilla, Mendoza Province, Argentina". *Tectonophysics* 836, page 229418. DOI: 10.1016/j.tecto.2022.229418.

Galland, O., S. Planke, E.-R. Neumann, and A. Malthe-Sørenssen (2009). "Experimental modelling of shallow magma emplacement: Application to saucer-shaped intrusions". *Earth and Planetary Science Letters* 277(3–4), pages 373–383. DOI: 10.1016/j.epsl.2008.11.003.

Galland, O., J. B. Spacapan, O. Rabbel, K. Mair, F. G. Soto, T. Eiken, M. Schiuma, and H. A. Leanza (2019). "Structure, emplacement mechanism and magma-flow significance of igneous fingers – Implications for sill emplacement in sedimentary basins". *Journal of Structural Geology* 124, pages 120–135. DOI: 10.1016/j.jsg.2019.04.013.

Gibson, M. E. and C. H. Wellman (2021). "The use of spore–pollen assemblages to reconstruct vegetation changes in the Permian (Lopingian) Zechstein deposits of northeast England". *Review of Palaeobotany and Palynology* 288, page 104399. DOI: 10.1016/j.revpalbo.2021.104399.

Heeremans, M. and J. I. Faleide (2004). "Late Carboniferous-Permian tectonics and magmatic activity in the Skagerrak, Kattegat and the North Sea". *Geological Society, London, Special Publications* 223(1), pages 157–176. DOI: 10.1144/gsl.sp.2004.223.01.07.

Henningsmoen, G. (1978). "Sedimentary rocks associated with the Oslo Region lavas". *Norges geologiske undersøkelse* 337, pages 17–24.

Jerram, D. A. and H. Stollhofen (2002). "Lava–sediment interaction in desert settings; are all peperite-like textures the result of magma–water interaction?" *Journal of Volcanology and Geothermal Research* 114(1–2), pages 231–249. DOI: 10.1016/s0377-0273(01)00279-7.

Larsen, B. T., S. Olaussen, B. Sundvoll, and M. Heeremans (2008). "The Permo-Carboniferous Oslo Rift through six stages and 65 million years". *Episodes* 31(1), pages 52–58. DOI: 10.18814/epiiugs/2008/v31i1/008.

Le Mével, H., P. M. Gregg, and K. L. Feigl (2016). "Magma injection into a long-lived reservoir to explain geodetically measured uplift: Application to the 2007–2014 unrest episode at Laguna del Maule volcanic field, Chile". *Journal of Geophysical Research: Solid Earth* 121(8), pages 6092–6108. DOI: 10.1002/2016jb013066.

Lefebvre, N., J. White, and B. Kjarsgaard (2012). "Spatter-dike reveals subterranean magma diversions: Consequences for small multivent basaltic eruptions". *Geology* 40(5), pages 423–426. DOI: 10.1130/g32794.1.

Lenhardt, N., S. M. Masango, O. O. Jolayemi, S. Z. Lenhardt, G.-J. Peeters, and P. G. Eriksson (2017). "The Palaeoproterozoic (2.06 Ga) Rooiberg Group, South Africa: Dominated by extremely high-grade lava-like and rheomorphic ignimbrites? New observations and lithofacies analysis". *Journal of African Earth Sciences* 131, pages 213–232. DOI: 10.1016/j.jafrearsci.2017.03.030.

Lindoo, A., J. Larsen, K. Cashman, and J. Oppenheimer (2017). "Crystal controls on permeability development and degassing in basaltic andesite magma". *Geology* 45(9), pages 831–834. DOI: 10.1130/g39157.1.

Lipman, P. W. (1976). "Caldera-collapse breccias in the western San Juan Mountains, Colorado". *Geological Society of America Bulletin* 87(10), page 1397. DOI: 10.1130/0016-7606(1976)87<1397:cbitws>2.0.co;2.

Lipman, P. W., M. J. Zimmerer, and W. C. McIntosh (2015). "An ignimbrite caldera from the bottom up: Exhumed floor and fill of the resurgent Bonanza caldera, Southern Rocky Mountain volcanic field, Colorado". *Geosphere* 11(6), pages 1902–1947. DOI: 10.1130/ges01184.1.

Liszewska, K. M., J. C. White, R. Macdonald, and B. Bagiński (2018). "Compositional and Thermodynamic Variability in a Stratified Magma Chamber: Evidence from the Green Tuff Ignimbrite (Pantelleria, Italy)". *Journal of Petrology* 59(12), pages 2245–2272. DOI: 10.1093/petrology/egy095.

Locchi, S., S. Zanchetta, and A. Zanchi (2022). "Evidence of Early Permian extension during the post-Variscan evolution of the central Southern Alps (N Italy)". *International Journal of Earth Sciences* 111(6), pages 1717–1738. DOI: 10.1007/s00531-022-02220-2.

Lutro, O. and Ø. Nordgulen (2008). *Oslofeltet. Berggrunnskart.* Norges geologiske undersøkelse. [Map scale 1: 250,000].

Magnall, N., M. R. James, H. Tuffen, and C. Vye-Brown (2017). "Emplacing a Cooling-Limited Rhyolite Lava Flow: Similarities with Basaltic Lava Flows". *Frontiers in Earth Science* 5. DOI: 10.3389/feart.2017.00044.

Manville, V., K. Németh, and K. Kano (2009). "Source to sink: A review of three decades of progress in the understanding of volcaniclastic processes, deposits, and hazards". *Sedimentary Geology* 220(3–4), pages 136–161. DOI: 10.1016/j.sedgeo.2009.04.022.

Manville, V. and C. J. N. Wilson (2004). "The 26.5 ka Oruanui eruption, New Zealand: A review of the roles of volcanism and climate in the post-eruptive sedimentary response". *New Zealand Journal of Geology and Geophysics* 47(3), pages 525–547. DOI: 10.1080/00288306.2004.9515074.

Martí, J. (1991). "Caldera-like structures related to Permo-Carboniferous volcanism of the Catalan Pyrenees (NE Spain)". *Journal of Volcanology and Geothermal Research* 45(3–4), pages 173–186. DOI: 10.1016/0377-0273(91)90057-7.

Martí, J., G. Groppelli, and A. Brum da Silveira (2018). "Volcanic stratigraphy: A review". *Journal of Volcanology and Geothermal Research* 357, pages 68–91. DOI: 10.1016/j.jvolgeores.2018.04.006.

Martin-Jones, C., C. Lane, M. Van Daele, T. V. D. Meeren, C. Wolff, H. Moorhouse, E. Tomlinson, and D. Verschuren (2019). "History of scoria-cone eruptions on the eastern shoulder of the Kenya–Tanzania Rift revealed in the 250-ka sediment record of Lake Chala near Mount Kilimanjaro". *Journal of Quaternary Science* 35(1–2), pages 245–255. DOI: 10.1002/jqs.3140.

Mattsson, T., S. Burchardt, B. S. G. Almqvist, and E. Ronchin (2018). "Syn-Emplacement Fracturing in the Sandfell Laccolith, Eastern Iceland—Implications for Rhyolite Intrusion Growth and Volcanic Hazards". *Frontiers in Earth Science* 6. DOI: 10.3389/feart.2018.00005.

McCann, T., C. Pascal, M. Timmerman, P. Krzywiec, J. López-Gómez, L. Wetzel, C. Krawczyk, H. Rieke, and J. Lamarche (2006). "Post-Variscan (end Carboniferous-Early Permian) basin evolution in Western and Central Europe". *Geological Society, London, Memoirs* 32(1), pages 355–388. DOI: 10.1144/gsl.mem.2006.032.01.22.

Mizera, T., P. Petrik, M. Dobias, Sklencar, Sab, E. A. Taşkın, N. Belgacem, M. Varga, M. Kuhn, P. Wells, and S. Natsis (2022). "lutraconsulting/input: Release 1.3.0". *Zenodo*. DOI: 10.5281/ZENODO.6375199. [Software].

Moore, I. and P. Kokelaar (1998). *Geological Society of America Bulletin* 110(11), page 1448. DOI: 10.1130/0016-7606(1998)110<1448:tcpcca>2.3.co;2.

Namiki, A. and M. Manga (2008). "Transition between fragmentation and permeable outgassing of low viscosity magmas". *Journal of Volcanology and Geothermal Research* 169(1–2), pages 48–60. DOI: 10.1016/j.jvolgeores.2007.07.020.

Naterstad, J. (1978). "Excursion 2. Nittedal cauldron (Alnsjøen area)". *The Oslo paleorift - A review and guide to excursions*, pages 99–104.

Navarrete, C., K. Butler, M. Hurley, and M. Márquez (2020). "An early Jurassic graben caldera of Chon Aike silicic LIP at the southernmost massif of the world: The Deseado caldera, Patagonia, Argentina". *Journal of South American Earth Sciences* 101, page 102626. DOI: 10.1016/j.jsames.2020.102626.

Neumann, E.-R., K. Olsen, and W. Baldridge (2006). "The Oslo rift". *Continental rifts: evolution, structure, tectonics*. Edited by K. H. Olsen. Elsevier, pages 345–373. ISBN: 9780444895660. DOI: 10.1016/s0419-0254(06)80017-0.

Neumann, E.-R., K. Olsen, W. Baldridge, and B. Sundvoll (1992). "The Oslo Rift: A review". *Tectonophysics* 208(1–3), pages 1–18. DOI: 10.1016/0040-1951(92)90333-2.

Neumann, E.-R., B. T. Larsen, and B. Sundvoll (1985). "Compositional variations among gabbroic intrusions in the Oslo rift". *Lithos* 18, pages 35–59. DOI: 10.1016/0024-4937(85)90005-2.

Neumann, E.-R., G. R. Tilton, and E. Tuen (1988). "Sr, Nd and Pb isotope geochemistry of the Oslo rift igneous province, southeast Norway". *Geochimica et Cosmochimica Acta* 52(8), pages 1997–2007. DOI: 10.1016/0016-7037(88)90180-9.

Neumann, E.-R., M. Wilson, M. Heeremans, E. A. Spencer, K. Obst, M. J. Timmerman, and L. Kirstein (2004). "Carboniferous-Permian rifting and magmatism in southern Scandinavia, the North Sea and northern Germany: a review". *Geological Society, London, Special Publications* 223(1), pages 11–40. DOI: 10.1144/gsl.sp.2004.223.01.02.

Oftedahl, C. (1946). "On Akerites, Felsites, and Rhomb Porphyries". *Studies on the Igneous Rock Complex of the Oslo Region* 1.

– (1978a). "Cauldrons of the Permian Oslo rift". *Journal of Volcanology and Geothermal Research* 3(3–4), pages 343–371. DOI: 10.1016/0377-0273(78)90043-4.

– (1978b). "Main Geologic Features of the Oslo Graben". *Tectonics and Geophysics of Continental Rifts* 37, pages 149–165.

Olaussen, S., B. Larsen, and R. Steel (1994). "The Upper Carboniferous-Permian Oslo Rift; Basin Fill in Relation to Tectonic Development". *Pangea: Global Environments and Resources*. Volume 17. CSPG Special Publications, pages 175–197.

Olerud, S. (2002). *Nannestad*. Norges geologiske undersøkelse. [Map scale 1: 50,000].

Palmer, B. A., A. M. Purves, and S. L. Donoghue (1993). "Controls on accumulation of a volcaniclastic fan, Ruapehu composite volcano, New Zealand". *Bulletin of Volcanology* 55(3), pages 176–189. DOI: 10.1007/bf00301515.

Palmer, B. A. and V. E. Neall (1991). "Contrasting lithofacies architecture in ring-plain deposits related to edifice construction and destruction, the Quaternary Stratford and Opunake Formations, Egmont Volcano, New Zealand". *Sedimentary Geology* 74(1–4), pages 71–88. DOI: 10.1016/0037-0738(91)90035-c.

Pedersen, L., L. Heaman, and P. Holm (1995). "Further constraints on the temporal evolution of the Oslo Rift from precise U-Pb zircon dating in the Siljan-Skrim area". *Lithos* 34(4), pages 301–315. DOI: 10.1016/0024-4937(94)00014-s.

Pinkerton, H. and L. Wilson (1994). "Factors controlling the lengths of channel-fed lava flows". *Bulletin of Volcanology* 56(2), pages 108–120. DOI: 10.1007/bf00304106.

QGIS Development Team (2009). *QGIS Geographic Information System*. (Version 3.28) [Computer software]. Open Source Geospatial Foundation. URL: http://qgis.org.

Ramberg, I. and B. Larsen (1978). "Tectonomagnetic evolution". *The Oslo Paleorift - A Review and Guide to Excursions*, pages 56–75.

Rämö, O. T., T. Andersen, and M. J. Whitehouse (2022). "Timing and Petrogenesis of the Permo-Carboniferous Larvik Plutonic Complex, Oslo Rift, Norway: New Insights from U–Pb, Lu-Hf, and O Isotopes in Zircon". *Journal of Petrology* 63(12). DOI: 10.1093/petrology/egac116.

Re, G., J. D. L. White, J. D. Muirhead, and M. H. Ort (2016). "Subterranean fragmentation of magma during conduit initiation and evolution in the shallow plumbing system of the small-volume Jagged Rocks volcanoes (Hopi Buttes Volcanic Field, Arizona, USA)". *Bulletin of Volcanology* 78(8). DOI: 10.1007/s00445-016-1050-3.

Repstock, A., R. Casas-García, M. Zeug, C. Breitkreuz, B. Schulz, H. Gevorgyan, F. Heuer, S. Gilbricht, and M. Lapp (2022). "The monotonous intermediate magma system of the Permian Wurzen caldera, Germany: Magma dynamics and petrogenetic constraints for a supereruption". *Journal of Volcanology and Geothermal Research* 429, page 107596. DOI: 10.1016/j.jvolgeores.2022.107596.

Rhodes, E. L., A. K. Barker, S. Burchardt, C. F. Hieronymus, S. N. Rousku, D. W. McGarvie, T. Mattsson, T. Schmiedel, E. Ronchin, and T. Witcher (2021). "Rapid Assembly and Eruption of a Shallow Silicic Magma Reservoir, Reyðarártindur Pluton, Southeast Iceland". *Geochemistry, Geophysics, Geosystems* 22(11). DOI: 10.1029/2021gc009999.

Rohrman, M., P. van der Beek, and P. Andriessen (1994). "Syn-rift thermal structure and post-rift evolution of the Oslo Rift (southeast Norway): New constraints from fission track thermochronology". *Earth and Planetary Science Letters* 127(1–4), pages 39–54. DOI: 10.1016/0012-821x(94)90196-1.

Ross, P.-S., I. Ukstins Peate, M. McClintock, Y. Xu, I. Skilling, J. White, and B. Houghton (2005). "Mafic volcaniclastic deposits in flood basalt provinces: A review". *Journal of Volcanology and Geothermal Research* 145(3–4), pages 281–314. DOI: 10.1016/j.jvolgeores.2005.02.003.

Ross, P.-S. and J. D. L. White (2005). "Mafic, Large-Volume, Pyroclastic Density Current Deposits from Phreatomagmatic Eruptions in the Ferrar Large Igneous Province, Antarctica". *The Journal of Geology* 113(6), pages 627–649. DOI: 10.1086/449324.

Sæther, E. (1946). "The area of sediments and Lavas in Nittedal". *Studies on the igneous rock complex of the Oslo region*. Volume 1.

– (1947). "The Dykes in the Cambro-silurian Lowland of Baerum". *Studies on the Igneous Rock Complex of the Oslo Region*.

– (1962). "General investigation of the igneous rocks in the area north of Oslo". *Studies on the igneous rock complex of the Oslo region*, pages 1–184.

Schneider, J.-L., A. Le Ruyet, F. Chanier, C. Buret, J. Ferrière, J.-N. Proust, and J.-B. Rosseel (2001). "Primary or secondary distal volcaniclastic turbidites: how to make the distinction? An example from the Miocene of New Zealand (Mahia Peninsula, North Island)". *Sedimentary Geology* 145(1–2), pages 1–22. DOI: 10.1016/s0037-0738(01)00108-7.

Schulmann, K., J.-B. Edel, J. R. Martínez Catalán, S. Mazur, A. Guy, J.-M. Lardeaux, P. Ayarza, and I. Palomeras (2022). "Tectonic evolution and global crustal architecture of the European Variscan belt constrained by geophysical data". *Earth-Science Reviews* 234, page 104195. DOI: 10.1016/j.earscirev.2022.104195.

Scoon, R. N. (2018). *Geology of National Parks of Central/Southern Kenya and Northern Tanzania*. Springer International Publishing. ISBN: 9783319737850. DOI: 10.1007/978-3-319-73785-0.

Segalstad, T. (1975). "Cauldron subsidences, ring-structures, and major faults in the Skien district, Norway". *Norsk Geologisk Tidsskrift* 55, pages 321–333.

Skilling, I., J. White, and J. McPhie (2002). "Peperite: a review of magma–sediment mingling". *Journal of Volcanology and Geothermal Research* 114(1–2), pages 1–17. DOI: 10.1016/s0377-0273(01)00278-5.

Sohn, C. and Y. K. Sohn (2019). "Distinguishing between primary and secondary volcaniclastic deposits". *Scientific Reports* 9(1). DOI: 10.1038/s41598-019-48933-4.

Sørensen, R. (1975). "The Ramnes Cauldron in the Permian of the Oslo Region, Southern Norway". *Norges Geologiske Undersøkelse Bulletin* 321, pages 67–86.

Stanistreet, I. G., C. Doyle, T. Hughes, E. D. Rushworth, H. Stollhofen, N. Toth, K. Schick, and J. K. Njau (2020). "Changing depocentre environments of Palaeolake Olduvai and carbonates as marker horizons for hiatuses and lake-level extremes". *Palaeogeography, Palaeoclimatology, Palaeoecology* 560, page 110032. DOI: 10.1016/j.palaeo.2020.110032.

Sumner, J. M. and M. J. Branney (2002). "The emplacement history of a remarkable heterogeneous, chemically zoned, rheomorphic and locally lava-like ignimbrite: 'TL' on Gran Canaria". *Journal of Volcanology and Geothermal Research* 115(1–2), pages 109–138. DOI: 10.1016/s0377-0273(01)00311-0.

Sundvoll, B., E.-R. Neumann, B. Larsen, and E. Tuen (1990). "Age relations among Oslo Rift magmatic rocks: implications for tectonic and magmatic modelling". *Tectonophysics* 178(1), pages 67–87. DOI: 10.1016/0040-1951(90)90460-p.

Sundvoll, B. and B. Larsen (1994). "Architecture and early evolution of the Oslo Rift". *Tectonophysics* 240(1–4), pages 173–189. DOI: 10.1016/0040-1951(94)90271-2.

Sundvoll, B., B. Larsen, and B. Wandaas (1992). "Early magmatic phase in the Oslo Rift and its related stress regime". *Tectonophysics* 208(1–3), pages 37–54. DOI: 10.1016/0040-1951(92)90335-4.

Swenton, V. M., M. J. Streck, D. P. Miggins, and W. C. McIntosh (2022). "Filling critical gaps in the space-time record of High Lava Plains and co-Columbia River Basalt Group rhyolite volcanism". *GSA Bulletin*. DOI: 10.1130/b36346.1.

Tian, W., I. H. Campbell, C. M. Allen, P. Guan, W. Pan, M. Chen, H. Yu, and W. Zhu (2010). "The Tarim picrite–basalt–rhyolite suite, a Permian flood basalt from northwest China with contrasting rhyolites produced by fractional crystallization and anatexis". *Contributions to Mineralogy and Petrology* 160(3), pages 407–425. DOI: 10.1007/s00410-009-0485-3.

Torsvik, T. H. and L. R. M. Cocks (2004). "Earth geography from 400 to 250 Ma: a palaeomagnetic, faunal and facies review". *Journal of the Geological Society* 161(4), pages 555–572. DOI: 10.1144/0016-764903-098.

Torsvik, T. H., M. A. Smethurst, K. Burke, and B. Steinberger (2008). "Long term stability in deep mantle structure: Evidence from the 300 Ma Skagerrak-Centered Large Igneous Province (the SCLIP)". *Earth and Planetary Science Letters* 267(3–4), pages 444–452. DOI: 10.1016/j.epsl.2007.12.004.

Troll, V. R., C. H. Emeleus, G. R. Nicoll, T. Mattsson, R. M. Ellam, C. H. Donaldson, and C. Harris (2019). "A large explosive silicic eruption in the British Palaeogene Igneous Province". *Scientific Reports* 9(1). DOI: 10.1038/s41598-018-35855-w.

Tuffen, H., M. R. James, J. M. Castro, and C. I. Schipper (2013). "Exceptional mobility of an advancing rhyolitic obsidian flow at Cordón Caulle volcano in Chile". *Nature Communications* 4(1). DOI: 10.1038/ncomms3709.

Tye, R. S. and J. M. Coleman (1989). "Depositional processes and stratigraphy of fluvially dominated lacustrine deltas; Mississippi delta plain". *Journal of Sedimentary Research* 59(6), pages 973–996. DOI: 10.1306/212F90CA-2B24-11D7-8648000102C1865D.

Valentine, G. A., D. Krier, F. V. Perry, and G. Heiken (2005). "Scoria cone construction mechanisms, Lathrop Wells volcano, southern Nevada, USA". *Geology* 33(8), pages 629–632. DOI: 10.1130/g21459ar.1.

Wadsworth, F. B., E. W. Llewellin, J. M. Castro, H. Tuffen, C. I. Schipper, J. E. Gardner, J. Vasseur, A. Foster, D. E. Damby, I. M. McIntosh, S. Boettcher, H. E. Unwin, M. J. Heap, J. I. Farquharson, D. B. Dingwell, K. Iacovino, R. Paisley, C. Jones, and J. Whattam (2022). "A reappraisal of explosive–effusive silicic eruption dynamics: syn-eruptive assembly of lava from the products of cryptic fragmentation". *Journal of Volcanology and Geothermal Research* 432, page 107672. DOI: 10.1016/j.jvolgeores.2022.107672.

Wadsworth, F. B., E. W. Llewellin, J. Vasseur, J. E. Gardner, and H. Tuffen (2020). "Explosive-effusive volcanic eruption transitions caused by sintering". *Science Advances* 6(39). DOI: 10.1126/sciadv.aba7940.

Waichel, B. L., E. F. de Lima, C. A. Sommer, and R. Lubachesky (2007). "Peperite formed by lava flows over sediments: An example from the central Paraná Continental Flood Basalts, Brazil". *Journal of Volcanology and Geothermal Research* 159(4), pages 343–354. DOI: 10.1016/j.jvolgeores.2006.07.009.

Walker, G. P. L. (1983). "Ignimbrite types and ignimbrite problems". *Journal of Volcanology and Geothermal Research* 17(1–4), pages 65–88. DOI: 10.1016/0377-0273(83)90062-8.

– (1984). "Downsag calderas, ring faults, caldera sizes, and incremental caldera growth". *Journal of Geophysical Research: Solid Earth* 89(B10), pages 8407–8416. DOI: 10.1029/jb089ib10p08407.

White, J. and B. Houghton (2006). "Primary volcaniclastic rocks". *Geology* 34(8), page 677. DOI: 10.1130/g22346.1.

White, J. D. L., J. McPhie, and I. Skilling (2000). "Peperite: a useful genetic term". *Bulletin of Volcanology* 62(1), pages 65–66. DOI: 10.1007/s004450050293.

Willcock, M., G. Bargossi, R. Weinberg, G. Gasparotto, R. Cas, G. Giordano, and M. Marocchi (2015). "A complex magma reservoir system for a large volume intra- to extra-caldera ignimbrite: Mineralogical and chemical architecture of the VEI8, Permian Ora ignimbrite (Italy)". *Journal of Volcanology and Geothermal Research* 306, pages 17–40. DOI: 10.1016/j.jvolgeores.2015.09.015.

Wolfenden, E., C. Ebinger, G. Yirgu, A. Deino, and D. Ayalew (2004). "Evolution of the northern Main Ethiopian rift: birth of a triple junction". *Earth and Planetary Science Letters* 224(1–2), pages 213–228. DOI: 10.1016/j.epsl.2004.04.022.

Zanchetta, G., R. Sulpizio, and M. Di Vito (2004). "The role of volcanic activity and climate in alluvial fan growth at volcanic areas: an example from southern Campania (Italy)". *Sedimentary Geology* 168(3–4), pages 249–280. DOI: 10.1016/j.sedgeo.2004.04.001.

Zimanowski, B., R. Büttner, P. Dellino, J. D. L. White, and K. H. Wohletz (2015). "Magma–Water Interaction and Phreatomagmatic Fragmentation". *The Encyclopedia of Volcanoes*. Edited by H. Sigurdsson. 2nd edition. Academic Press, pages 473–484. DOI: 10.1016/B978-0-12-385938-9.00026-2.